People's Democratic Republic of Algeria

Ministry of Higher Education and Scientific Research

Echahid Hamma Lakhdar University of El-Oued

FACULTY OF TECHNOLOGY

MECHANICAL ENGINEERING DEPARTMENT

END OF CYCLE PROJECT

APPLIED FOR GRADUATION

ACADEMIC MASTER

FIELD: SCIENCE AND TECHNOLOGY

DEPARTMENT: MECHANICAL ENGINEERING

SPECIALIZATION: RENEWABLE ENERGIES

Theme

Design of fatigue testing machine for small wind turbines

Before the jury composed of:

Pr. Attia Abdelmalek	President
Mr. Bousbia Salah Seif eldin	Examiner
Dr. Gherbi Mohammed Taher	Supervisor
Mr. Khalil Deghoum	Supervisor assistant

Presented by:

Hemici Youcef

Academic year: 2022-2023

بِسْمِ اللهِ الرَّحْمنِ الرَّحِيمِ

وَاللَّهُ أَخْرَجَكُم مِّن بُطُونِ أُمَّهَاتِكُمْ لَا تَعْلَمُونَ شَيْئًا وَجَعَلَ لَكُمُ السَّمْعَ وَالْأَبْصَارَ وَالْأَفْئِدَةَ ۙ لَعَلَّكُمْ تَشْكُرُونَ"

سورة النحل الآية 78

ABSTRACT

Wind energy is considered one of the most important renewable energy sources. For this reason, researchers and experts have focused greatly on developing and improving it in all aspects. One of the challenges that receives special attention is the phenomenon of fatigue, which represents a major challenge in the field of wind energy and requires intensive efforts to address it and deal with its impact.

Based on previous research and studies, and as a way to materialize the idea, we designed a small device in this note to measure the voltage and bearing of wind turbine blades. This device allows results to be obtained by applying varying intensity forces to the studied blade, taking into account the materials and materials used in the manufacturing process.

We tested the machine through simulation, which allowed us to apply different loads to study stresses and displacements. To achieve this, we followed a few steps, including masking the parts that are constantly changing, which allowed us to monitor the stresses on the fixed parts. Deformation is also one of the causes that cause damage to mechanical parts and cause them to lose their functions.

الملخص

طاقة الرياح تعتبر واحدة من أهم مصادر الطاقة المتجددة. لهذا السبب، ركز الباحثون والخبراء بشكل كبير على تطويرها وتحسينها من جميع الجوانب. واحدة من التحديات التي تلقي اهتماماً خاصًا هي ظاهرة التعب، التي تمثل تحديًا كبيرًا في مجال طاقة الرياح وتتطلب جهودًا مكثفة لمعالجتها والتعامل مع تأثيرها.

باستنادًا إلى البحوث والدراسات السابقة، وكوسيلة لتجسيد الفكرة، قمنا بتصميم جهاز صغير في هذه المذكرة لقياس الجهد وتحمل شفرات توربينات الرياح. يتيح هذا الجهاز الحصول على نتائج من خلال تطبيق قوى متنوعة بكثافة على الشفرة المدروسة، مع مراعاة الخامات والمواد المستخدمة في عملية التصنيع.

قمنا بإجراء اختبار على الالة من خلال المحاكاة، والتي سمحت لنا بتطبيق أحمال مختلفة لدراسة الضغوط والازاحة. لتحقيق ذلك، اتبعنا بعض الخطوات، بما في ذلك إخفاء الأجزاء التي تتعرض للتغيير المستمر، مما سمح لنا بمراقبة الضغوط على الأجزاء الثابتة. كما أن التشوه يعتبر واحداً من الأسباب التي تسبب ضررًا للأجزاء الميكانيكية وتسبب في فقدان وظائفها.

DEDICATION

I dedicate my graduation to the person who taught me the value of generosity, and to the one whose name I proudly carry. May God grant you a long life, so you may witness the fruition of patiently awaited accomplishments, my dear father. I also dedicate this to my guiding angel, representing love, tenderness, and devotion, as well as the joy of living and the essence of existence. My beloved mother, whose prayers were the secret to my success, deserves special recognition. I extend my gratitude to the person who greatly contributed to my encouragement and motivation, teaching me the virtues of persistence and diligence. I have grown and relied upon this individual, gaining immeasurable strength and love from their presence. My brothers and sisters, with whom I discovered the true meaning of life, and those who exhibited loyalty and selflessness, deserve a dedicated tribute. I also acknowledge my dear friends, who shared both the joys and sorrows of life's journey and stood by me in the pursuit of success and goodness. With the grace of God and the support of my mother's prayers, I am only a few steps away from completing my academic journey. I express my gratitude to everyone who offered me a helping hand

ACKNOWLEDGMENT

First of all, our most sincere and warm thanks go to ALLAH Almighty who allowed us to be what we are today, and gave us the courage and health to complete this work.

Next, after that, we thank the administrative staff and the discussion committee for accepting this memorandum and the supervising professor,

Dr. **Gherbi Mohammed Taher**. I also extend special thanks and appreciation to the supervisor's assistant " **Mr. Khalil Deghoum** ", who enlightened me the way with his invaluable advice and guidance during my project.

List of figures

CHAPTER I

CHAPTER II

CHAPTER III

List of Abbreviations

HAWT: Horizontal Axis Wind Turbine.

VAWT: Vertical-axis wind turbine.

ASTM: American Society for Testing and Materials.

TLP: tension-leg platform.

FOWT: Floating Offshore Wind Turbines.

ASME: American Society of Mechanical Engineers.

LT: Leakage testing.

TSR: the tip speed ratio.

FET: field effect transistor.

UFET: external voltage.

Symbol

b	coefficient expressing the effect of repeated stress on failure.
C&n	constants representing material properties and crack growth velocity.
d1 d2 d3 R m	rainflow range.
x_m	normalized mean frequency.
γ	irregularity factor.
Z	normalized variable.
K	The quantity of load groups that have been imposed on the component**.**
λ	the process variable of a PI-controller

Table of Contents

GENERAL INTRODUCTION

Wind turbines are an important technology in renewable energy generation, used to convert wind energy into clean and sustainable electrical energy. This technology is an essential part of efforts to combat climate change and improve energy sustainability. As wind turbines develop and increase in size and power, this technology faces certain challenges, the most prominent of which is the problem of fatigue. Fatigue in this context refers to wear and stress resulting from the effects of wind and repetitive loading on turbine components.[1]

The problem of fatigue in wind turbines is an engineering challenge as it can reduce the useful service life of the turbine and increase maintenance costs. This problem includes material corrosion, the effects of strong winds and changes in wind speed, and the effects of vibration and repetitive loading on vital parts of the turbine.[2]

To address the problem of fatigue in wind turbines, researchers and engineers are conducting ongoing studies and research to develop corrosion-resistant materials and improve turbine designs and maintenance systems. Interests also include technologies for early detection and diagnosis of fatigue problems to increase wind turbine operating efficiency and maximize their utility.[3]

There are many studies and researchers who have researched the field of mechanical fatigue over the years. It is difficult to specifically identify the most famous of them all, but some prominent names and important research in this field can be mentioned:

- ✓ Claude Bathias: A famous French researcher in fatigue mechanics and materials engineering. He made many contributions to understanding the phenomenon of mechanical fatigue.[4]
- ✓ Alan Fatigue: American researcher and mechanical engineer famous for his work in the field of mechanical fatigue and dynamic load-oriented design.[5]
- ✓ Claude Louis Marie Henri Navier: Navier's experience in fatigue mechanics was his development of equations known as the Navier-Stokes equations that describe fluid flow.[6]
- ✓ August Wöhler: He conducted important experiments on the effect of mechanical changes on metallic materials, and developed the concept of fatigue limits and elastic limits.[7]
- ✓ Augustin-Louis Cauchy: He worked on developing important mathematical theories to describe deformation and fatigue in materials.[8]
- ✓ Paul Paris : He contributed to the development of the Paris law model, which is used to estimate the speed of crack development in fatigued materials.[9]

These are some of the leading figures in the field of mechanical fatigue. It is worth noting that there are many other researchers and scientists who have done important research in this field, and progress in this field continues continuously with the contributions of current researchers.

CHAPTER I

INTRODUCTION TO MODERN WIND TURBINES

I. Introduction

Unrestricted access to electrical power stands as a crucial catalyst for the ongoing advancement of nations and societies. From the outset of the twentieth century, fossil fuels have functioned as the predominant energy source, fueling the rapid progression of civilization. Nonetheless, due to environmental and economic concerns, numerous countries are implementing fresh regulations aimed at curbing the utilization of fossil fuels and the resultant CO2 emissions[10-12]. In accordance with these directives, most nations have committed to augmenting the proportion of renewable energy generation within their overall installed electrical capacity. Wind power emerges as a promising substitute for fossil fuels, as it holds the potential to diminish fossil fuel consumption and emissions of exhaust gases. The primary drawback associated with wind power lies in its pronounced susceptibility to meteorological conditions[13, 14]. This drawback renders the production of wind energy challenging to manage and predict. Additional disadvantages encompass the audible noise generated by wind turbines, as well as their visual intrusion, and their environmental consequences, including their impact on local ecosystems, particularly on avian species.[15, 16]

Vertical axis wind turbines (VAWT) are better suited for urban settings due to several factors. These include reduced noise generation, higher wind speed requirements for operation, lower minimum wind speed needs, resistance to wind turbulence, capability to harness wind from all directions, and a compact design[17, 18]. Consequently, there is a growing research interest, encompassing both experimental and numerical approaches, in the field of VAWT. Nevertheless, there is still much ground to cover to reach a level of development comparable to horizontal axis wind turbines (HAWT).

Horizontal axis wind turbines (HAWT) possess numerous advantages over their vertical axis wind turbine (VAWT) counterparts. These advantages include heightened efficiency and scalability, as well as the ability to maintain consistent performance by operating at a stable rotational speed, unlike VAWT that may encounter varying rotational speeds. Additionally, the increased height of HAWT substantially enhances their power generation capabilities. HAWT are equipped with a yaw system that automatically positions them to face the wind, thereby optimizing energy capture. Notably, maintenance accessibility is a key advantage, as HAWT systems can enjoy a prolonged operational lifespan, often surpassing 20 years.[19, 20]

II. Types and classifications of wind turbines

By definition, a wind turbine is a machine that transforms wind kinetic energy into useful mechanical power that may be used to produce electricity. Vertical axis wind turbines (VAWT) and horizontal-axis wind turbines are the two different types of wind turbine systems, which may be distinguished by the way the blades look from the outside (HAWT)[21]

Figure I. 1: The two types of wind turbines in terms of the way they rotate and the difference between them[22]

II.1 Vertical axis wind turbines

vertical-axis wind turbines (VAWT) can gather winds from any direction because their axis of rotation is vertical. Because they don't rely on the direction of the wind, vertical-axis wind turbines were also used in some applications. Power can be taken out significantly more easily.[23]

The main rotor shaft of vertical-axis wind turbines (or VAWT) is positioned vertically Figure The fact that the turbine does not have to be pointed into the wind in order to function is a benefit of this setup for locations where the wind direction is highly variable. The turbine is less steerable by nature when it is integrated into a building, which is another benefit. Also, by adopting a direct drive from the rotor assembly to the ground-based gearbox, the generator and gearbox can be positioned close to the ground, boosting accessibility for maintenance. Unfortunately, these designs generate far less energy on average over time, which is a significant disadvantage.[24]

II.1.1 Savonius Wind Turbine

Anemometers, Flettner vents (often seen on bus and van roofs), and some high-reliability low-efficiency power turbines all use these drag-type components with two (or more) scoops. If there are at least three scoops, they always self-start. A savonius that has been modified to include lengthy helical scoops for smooth torque is known as twisted savonius. This may even be used on ships and is frequently utilized as a rooftop wind turbine [25]

Figure I. 2: Savonius wind turbine**[**26]

In 2013, New Wind unveiled its prototype. After trying out several potential designs, the company settled on an arrangement of paper turbines on each branch that might seem chaotic at first glance. The latest version of this innovative creation is less than 30 feet long and 23 feet wide. It includes 54 paper turbines capable of capturing up to 5.4 kilowatts of energy at a time and producing approximately 2,400 kilowatt-hours per year. This is equivalent to powering a small, low-consumption office for 12 months or charging an electric car for 10,000 miles per year, saving About 160 gallons of fuel.

Introduced to the public in December 2015 by French company New Wind, the Wind Tree is an impressive vertical wind turbine designed to resemble a tree. Measuring less than 30 feet high and spanning 23 feet wide, this innovative structure houses 54 leaf-shaped turbines that operate silently, efficiently harnessing energy from winds at speeds less than 5 mph, and generating up to 5.4 kilowatts of power per revolution. On an annual basis, the Wind Tree has the capacity to produce 2,400 kilowatt

hours of electricity, enough to power a home. Moreover, its visual aesthetics contribute to its overall appeal.[27]

Figure I. 3: Wind trees[28]

It embodies artistic expression while also representing an advancement in sustainable development. However, the current form of trees falls short of being a long-term or widely applicable solution due to their impracticality for household use—being heavy, space-consuming, and costly. To illustrate, a single wind tree, priced at approximately 49,500 euros (equivalent to $56,000) including delivery and installation, is significantly more expensive than solar alternatives. Solar photovoltaic panels with a similar energy output (5.4 kilowatts) range from 15,000 to 20,000 euros ($17,000 to $22,600) in France, according to data from the country's Environment and Energy Agency.[27]

II.1.2 Darrieus Wind Turbine

Georges Darrieus, a French inventor, is the namesake of the "Eggbeater" or Darrieus turbines [Ver 13]. Despite their high torque ripple and cyclical stress on the tower, they are highly efficient but have poor reliability. Also, because of their extremely low starting torque, they frequently need an additional Savonius rotor or external power source to turn. Using three or more blades increases the rotor's robustness while reducing torque ripple[29].

By dividing the blade area by the rotor area, solidity is calculated. In more recent Darrieus type turbines, the top bearing is connected to an exterior superstructure rather than guy wires An illustration of a vertical axis wind turbine (VAWT) [30]

Figure I. 4: Types of Darrieus wind turbines[31]

Several approaches have been suggested to enhance the energy efficiency of Savonius turbines. the most effective strategy for improving both power output and the turbine's ability to self-start involves reducing fluid resistance on the returning blade and increasing fluid pressure on the leading blade. demonstrates that these effects can be achieved through various adjustments, such as altering blade angles, modifying blade shapes, adjusting the number of stages, optimizing aspect ratios, and managing overlap ratios. Savonius turbines find applications primarily in wind and water turbine contexts.

II.2 Horizontal axis wind turbines

They are the most common type of wind turbine. It can be defined as a turbine whose rotor shaft is in the direction of the wind as shown in the figure. [32]

Figure I. 5: Horizontal axis wind turbines[33]

The blades are aerodynamically designed which rotate by the aerodynamic lift of force. A pressure difference is created between the upper and lower faces of the turbine blades. As a result of the rotor shaft's meshing with the generator, electricity is produced by rotating the rotor shaft. This type of turbine often uses a wind sensor and servo motor to ensure that the rotor blades are facing the wind. The wind turbine is equipped with a brake to lower rotor shaft speed since high wind speeds could be hazardous and could harm the device [34].

Wind turbines can be single-bladed(a), double-bladed(b) or three-bladed(c)

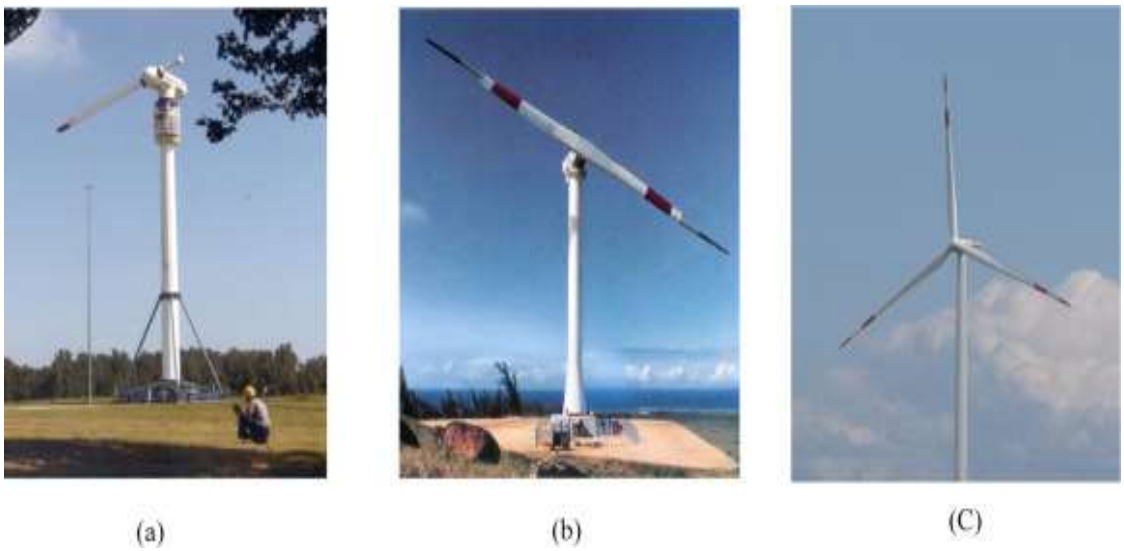

Figure I. 6: The main types of horizontal axis wind turbines[33]

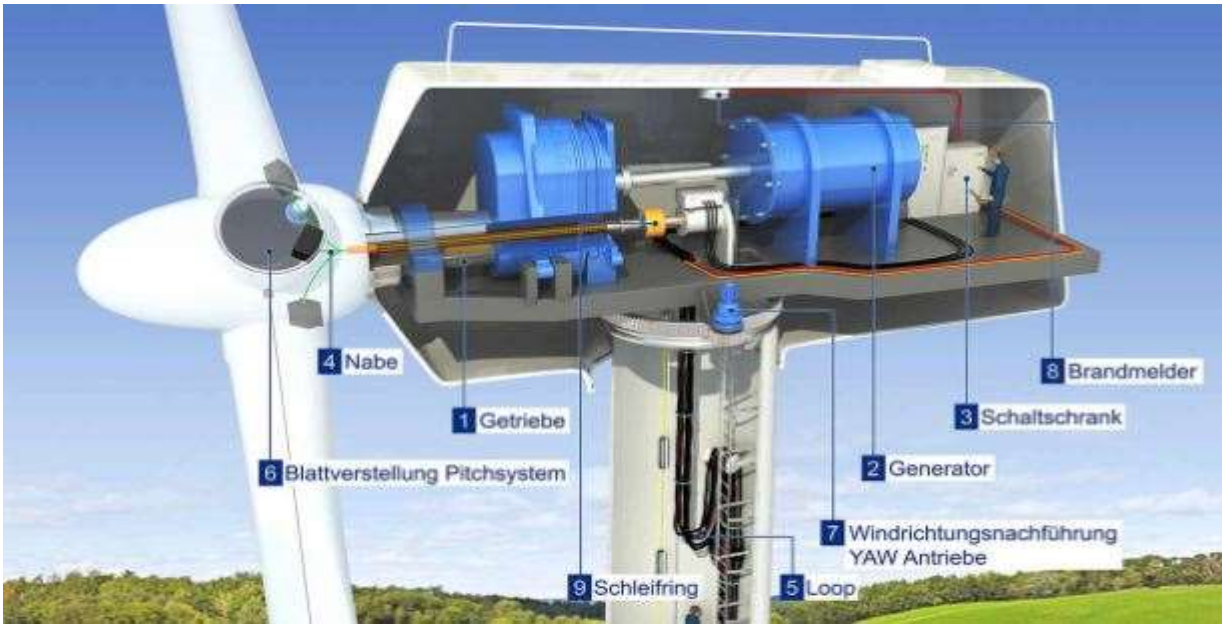

Figure I. 7: Cross section of a vertical wind turbine[35]

Data acquisition and turbine control are managed through a real-time controller, the National Instruments cRIO-9074. Both analog and counter-based data, including rotational velocity, are captured in perfect synchronization, allowing for the adjustment of two distinct sampling frequencies. Typically, analog data is recorded at a rate of $f_s \leq 10$ kHz, depending on the specific application. However, when measuring rotational speed, a trade-off between speed and accuracy is essential. In this case, a satisfactory outcome was achieved by limiting the sampling rate of ω to 200 Hz.[1]

The closed-loop load control of the model wind turbine is achieved using a field effect transistor (FET) within the electric circuit. By applying an external voltage U_{FET} to the transistor, the electric load is varied and the torque becomes adjustable. The closed-loop control is based on a reference velocity upstream of the rotor as the tip speed ratio (TSR) λ is the process variable of a PI-controller, and there with the constant set point. The manipulative variable is the voltage U_{FET}, altering the torque. With this approach, the model turbine automatically reacts to changing inflow conditions, keeping its TSR constant, which allows convenient, time efficient and reproducible experiments.

Figure I. 8: 5M wind turbine off the coast of Belgium[36]

A relatively new but growing application of large-scale wind turbines is as units in offshore wind power stations. Figure shows the first wind turbines in a planned 300-MW offshore power station 30 km off the Belgium coast. These REpower Model 5M wind turbines, each of which has a rated power of 5.0 MW and a rotor diameter of 126 m, are installed in water 25 m deep.

In harsh marine conditions, moving parts are more likely to wear out. But by applying direct drive technology, Siemens Gamesa Offshore Direct Drive wind turbines use fewer moving parts than devices with similar gears. Besides reducing the potential for breakdowns, this also means that fewer spare parts are needed over the life of the wind farm. This unique combination of simplicity, durability and low weight significantly reduces infrastructure, installation and service costs - while maximizing energy production over the life of the project. Reduced payload simply translates to greater power output with lower life cycle cost[37]

Figure I. 9: Floating platform concepts for offshore wind turbines[38]

As shown in Figure, FOWTs can be divided into three basic categories: tension-leg platform (TLP), spar-buoy, and semisubmersible. Each of these floater designs differs in terms of how their weight, buoyant force, and mooring line forces interact to stabilize the platform. Each has advantages and disadvantages. The tension leg platform lowers the platform below its natural floating equilibrium position by using tensioned mooring lines. [39]

When disturbed, this tension works to turn the platform. Many businesses, like Glosten Associates (PelaStar), are already making substantial advancements in the testing and development of TLP-based floating wind turbines.[40]

In order to provide a moment of righting when upset, the spar-buoy places the center of gravity considerably below the center of buoyancy. Hywind, the world's first commercial-scale FOWT, was deployed by Statoil en 2009 This 2.3 MW spar-buoy mounted turbine served as a research test site and produced data that would help with their next project to build a wind farm with 3-5 turbines. Two 7 MW turbines will be placed on their current wind energy testing grounds as part of the second phase of the Fukushima Forward project [41] A floating tower that is submerged by a single tension leg and swivel makes up the SWAY floating wind turbine, which combines a TLP and a spar buoy [42].

The buoyant force acting on the semisubmersible platform, which causes a righting moment and stabilizes the platform when disturbed, is distributed across a vast area by the platform's large footprint. From the earliest conceptual stages of development to the full-scale deployment of power-generating units, semisubmersible types are available. A semisubmersible concept called WindSea is still in its

infancy. WindSea has a tri floater architecture, like many semisubmersibles, however this platform is meant to host three different wind turbines instead of the typical one. For the purpose of validating performance and assisting in full scale design, WindSea has tested scale models in wind, wave, and wind-wave 5 conditions. [43]

III. Fatigue and mechanical testing

III.1 Machine fatigue

typically refers to the wear and tear that machines and mechanical components experience over time due to repeated use, stress, and exposure to various environmental factors. It is a common issue in engineering and industrial settings. Machine fatigue can lead to a decrease in performance, increased maintenance requirements, and, ultimately, mechanical failures if not properly managed and addressed.[44]

Figure I. 10: Fatigue Testing Machines[44]

III.2 Types of mechanical tests - measuring the strength of materials

Mechanical testing comprises a set of examinations employed in the realm of product design and component fabrication to ascertain, define, choose, and verify materials. Consequently, manufacturers can ascertain the suitable material usage, ensure safety during production, and achieve cost-efficiency. In this article, we will introduce these testing procedures and elucidate their roles in product design and the manufacturing of components.[44]

III.2.1 Torsion test

Torsion testing is another form of mechanical testing that evaluates the behavior of a material when subjected to compression at an angular displacement. As a result, it gives information about the material's shear modulus of elasticity, shear yield strength, shear strength, shear modulus of rupture, and ductility. Unlike tensile testing, torsion testing applies to materials and products. Moreover, there are several types which are described below.[44]

Figure I. 11: Torsional stress testing machine[45]

- Torsion only: Applying only a torsional load to the material
- Axial torsion: The application of axial (tension/compression) and torsional force to a material.
- Failure testing: Twisting a product or material until it breaks or a visible defect appears.
- Proof test: Applying a torsional load to the material and holding the torque for a certain time.
- Functional testing: The final test to verify the behavior of the material under torsional forces and loads

III.2.2 Fatigue test

Mechanical stress testing is used to assess the performance of a material when subjected to varying loads applied either axially, through twisting, or by bending. This process entails exposing the material to a combination of a constant load and a fluctuating load. Consequently, the material may undergo fatigue, which is when it eventually fails.

The data obtained from this testing is typically represented in an SN plot. This plot illustrates the relationship between the number of cycles required to induce failure and the amplitude of cyclic stress. This cyclic stress can be expressed as stress amplitude, maximum stress, or minimum stress.[44]

Figure I. 12: High strength fatigue testing machine[45]

III.2.3 Tensile test

Tensile testing is a fundamental mechanical strength assessment utilized to ascertain material characteristics like stress, strain, and yield deformation. This procedure entails applying opposing forces to a material, gradually pulling it until it fractures.

The examination is carried out employing a tensile testing machine, whether hydraulic or electric. The operator administers various forces to the material and documents the resulting data. Subsequently, they chart the data to generate a stress-strain curve on a graph. Widely recognized standards for conducting tensile tests encompass ASTM D638/ISO 527-2 (pertaining to reinforced plastics), ASTM D412/ISO 37 (concerning vulcanized rubber and thermoplastic elastomers), and ASTM E8/ASTM A370/ISO 6892 (applicable to metals and other metallic materials).[44]

Figure I. 13: Tensile testing machine[45]

III.2.4 Pressure test

Compression testing stands as a fundamental mechanical engineering examination used to ascertain how materials respond under crushing forces. Consequently, it holds significant importance in the realm of manufacturing, as materials undergo distinct phases during this process. This testing method is applicable to a diverse range of materials, including metals, plastics, ceramics, and other heavy-duty substances.

Well-established standards for compression testing encompass ASTM D3574 (pertaining to flexible cellular materials), ASTM D695-15 (for rigid plastics), AITM 0010, ASTM C109 (for 2-inch concrete cubes), and ISO 844 (pertaining to rigid cellular plastics).[44]

Figure I. 14: Pressure testing machine[45]

III.2.5 Fracture mechanics testing

Fracture mechanics testing enables manufacturers to assess the energy required to fracture a material that already contains a crack. Additionally, it provides a means for manufacturers to evaluate the material's capacity to withstand cracking under internal stress conditions. By analyzing the data obtained, manufacturers can investigate aspects such as brittle fracture, grain size, case depth, and more.

Figure I. 15: Fracture mechanics testing machine[45]

III.2.6 Corrosion resistance

Corrosion tests are accelerated tests to determine the reactions of coated and uncoated metals in salty and non-saline conditions. There are several types of tests according to international standards. Check out popular tests.[44]

- Salt spray test: This is the standard and most common method for checking the corrosion resistance of coated and uncoated materials. It involves spraying the material with a brine solution and evaluating the oxide appearance.
- CASS Exposure Test: This is an aggressive corrosion test for aluminum alloy and chrome plating on zinc and steel materials. It involves exposing the material to a copper-precipitated acetic acid salt spray. Moreover, the test can be functional or aesthetic, and determines the exposure time (no more than 48 hours).
- Immersion Corrosion Test: Immersion corrosion testing involves immersing a material in an aggressive water environment. Next, analytical methods are used to determine weight loss due to corrosion.

III.2.7 Leakage test (LT)

Leakage testing, often abbreviated as LT, comprises a series of examinations aimed at detecting the existence of fissures or any openings that may permit product leakage. These tests encompass four primary methods for detecting leaks: the bubble leak test, pressure variation test, halogen diode test, and mass spectrometer test.[44]

IV. Conclusion

When delving into the realm of mechanical fatigue machines, one discovers that this domain constitutes an integral segment of mechanical and materials engineering. Grasping the responses of materials to repeated stressors and environmental factors assumes a pivotal role in shaping the design and upkeep of mechanical components and structures. Numerous industries lean on these investigations to guarantee the safety and durability of their products.[46]

With the advent of technological progress, mechanical fatigue challenges are burgeoning across a spectrum of applications. Consequently, it becomes progressively imperative to persist in research and development endeavors aimed at enhancing our comprehension of mechanical processes and forging novel approaches for identifying and mitigating fatigue. By immersing ourselves in the study of mechanical fatigue machines, we elevate performance, efficiency, and dependability within the realm of engineering and industry.[47]

CHAPTER II

FATIGUE OF WIND TURBINE BLADE

I. Introduction

Mechanical fatigue is a fundamental phenomenon that occurs in materials subjected to cyclic loading or repeated stress. It refers to the progressive and localized structural damage that develops over time when a material undergoes alternating or fluctuating loads. Fatigue failure can be catastrophic, often occurring unexpectedly and leading to significant damage or even complete structural collapse.

The concept of mechanical fatigue has far-reaching implications in various fields of engineering and materials science, including aerospace, automotive, civil, and mechanical engineering. It affects the performance and reliability of a wide range of components and structures, such as aircraft wings, automobile frames, bridges, and machine parts.[48]

The fundamental cause of mechanical fatigue lies in the initiation and propagation of microscopic cracks within the material. These cracks typically form at locations of high stress concentration, such as notches, geometrical discontinuities, or material defects. Under cyclic loading, these cracks progressively grow and interact with each other, eventually leading to a macroscopic failure, even under stresses significantly lower than the material's ultimate strength.

Several factors influence the occurrence and progression of mechanical fatigue. The magnitude, frequency, and duration of the applied cyclic loads, along with the material's mechanical properties, play a crucial role. Additionally, environmental conditions, such as temperature, humidity, and corrosive agents, can significantly accelerate the fatigue process.[49]

Understanding and predicting mechanical fatigue behavior is vital for ensuring the structural integrity and safety of engineered systems. Engineers employ various techniques and methodologies to assess fatigue life and develop design strategies to mitigate fatigue failure. These include fatigue testing, stress analysis, fracture mechanics, and the use of fatigue design codes and standards.[50]

Advancements in materials science and engineering have led to the development of high-strength alloys, composites, and surface treatments that exhibit improved resistance to fatigue. However, the design and optimization of fatigue-resistant structures remain a complex challenge due to the diverse and intricate nature of cyclic loading conditions and the inherent variability of material behavior.[51]

In conclusion, mechanical fatigue is a critical phenomenon that affects the durability and reliability of materials and structures subjected to cyclic loading. Its understanding and mitigation are of paramount importance in engineering design, as it helps prevent catastrophic failures and ensures the safety of various applications. Ongoing research and technological advancements continue to enhance our knowledge and capabilities in managing and extending the fatigue life of engineered systems.[52]

II. Metal Fatigue – Wöhler Plot and Mechanisms

Assessing the fatigue durability or lifespan of specific metals is vital for advancing material choices and design procedures. Consequently, similar to other mechanical attributes and modes of failure, fatigue characteristics can be emulated using dedicated apparatus. Conventional testing equipment applies both compressive and tensile forces to the metal to replicate a fatigue sequence. This replication of the fatigue cycle is upheld through cyclic application of the tensile and compressive loads. Furthermore, to ensure dependable outcomes from the test, testing parameters (stress magnitude, stress amplitude, and frequency) are aligned with the operational conditions the tested material will encounter.[53]

To predict the anticipated operational duration of a substance or component exposed to recurrent stress, this equation was formulated by German materials researcher August Wöhler during the mid-1800s. It has undergone refinement and enhancement over successive eras [54]. While the equation is available in various formats, its fundamental structure adheres to the subsequent pattern:

$$\mathrm{Nf} = \left(\frac{\sigma a}{Kf}\right)^{b} \tag{II.1}$$

where:

N_f : the number of times the stress is repeated until failure occurs.

σa : the peak (maximum) stress to which the material is subjected during one cycle of stress.

K_f : the fatigue modulus of a material and it is a constant that represents the fatigue properties of that material

The values of Kf and b can be determined by repeated fatigue and stress tests of the material in question. Once the values of σa, Kf, and b are known, the equation can be used to estimate the number of times the stress is repeated until failure.

The use of the Wheeler-Fuller equation depends on assumptions related to the surrounding conditions and material properties, and note that there are other factors that may affect the actual service life of materials such as deformations, environmental conditions, engineering design, and others.

Fatigue life determination tests are carried out using stress levels that are typically set at around 66% of the material's tensile strength. The test involves subjecting specimens to stress cycles until they fail. If a sudden fracture occurs in a specimen, the stress applied to subsequent specimens is reduced. The stress level and fatigue cycles are recorded for each new specimen and used for analysis. The experimental data is then utilized to construct an S-N diagram, where S represents the maximum stress

or stress amplitude, and N represents the cycles to failure. This S-N diagram enables the estimation of the fatigue life of a specific metal at particular stress amplitudes. Decreasing the applied stress value leads to an increase in the number of cycles required for failure.[55]

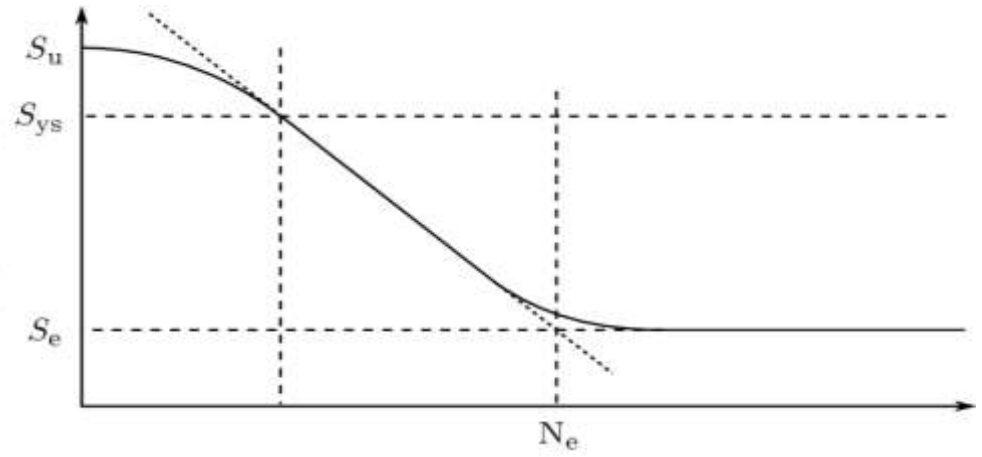

Figure II. 1: Typical behavior of the Wöhler curve of a steel, in log-log scale [56]

The typical behavior of the Wöhler curve for steel is depicted. It is important to note that this graph is presented on a bi-logarithmic scale. When the alternating stress is below Se, it can be considered that fatigue does not occur (in reality, the rate of fatigue damage abruptly slows down when Sf becomes lower than Se). This threshold defined by Se is known as the endurance limit.

III. Paris-Erdogan Law

It is an equation used in materials engineering and fatigue science to estimate the rate of crack growth (cracks) in materials subjected to repeated stress. This equation was jointly developed by French materials scientists Michel Paris and Turkish T.H. Erdogan in the 1970s.

The equation takes the following form:

$$\frac{da}{dN} = \mathrm{C} * \Delta \mathrm{K}^{n} \qquad \text{(II.2)}$$

Wher:

da/dN: is the rate of crack growth in each repetitive stress cycle.

ΔK: is the stress intensity variation across the flat at a given stage.

This equation provides a model for the velocity of crack growth through the material with changes in the stress intensity across the flat. This equation enables engineers and materials scientists to estimate the remaining service life of materials subjected to repeated fatigue and stress.

IV. Explaining a charging cycle

Although the purpose of this chapter is to discuss variable amplitude fatigue analysis, it is best to explain certain concepts using constant amplitude loading as an example. Let us take into account a uniaxial loading described by the equation:[57]

$$S(t) = S_a \sin(\omega t) + S_m \quad \text{(II.3)}$$

The maximum stress value S_{max} and the minimum stress value S_{min} make it possible to express the alternating component S_a and the average component S_m of a loading cycle:

$$S_a = \frac{\Delta S}{2} = \frac{S_{max} - S_{min}}{2} \quad \text{(II.4)}$$

$$S_m = \frac{S_{max} + S_{min}}{2} \quad \text{(II.5)}$$

ΔS*:* is the extent of the loading cycle.

$$R_s = \frac{S_{min}}{S_{max}} \quad \text{(II.6)}$$

Each point corresponding to S_{min} or S_{max} in a loading signal represents an inversion point where the derivative dS/dt is zero. When loading exhibits variable and random amplitude, each loading cycle exhibits a specific combination of S_{min} and S_{max} is used to assess fatigue damage. Fatigue does not occur when the specimen is under compression load [58]

Fatigue only occurs when dS/dt > 0 and S > 0.

In a theoretical analysis of uniaxial fatigue, it is necessary to remove the negative part of the stress signal. Therefore, if $S_{min} < 0$, we must consider $\Delta S = S_{max}$ and $R_s = 0$.

The fatigue process of a material can be divided into two distinct phases: crack initiation and crack propagation. Therefore, it is possible to describe this process as follows:

$$N_f = N_{in} + N_{pr} \quad \text{(II.7)}$$

$\boldsymbol{N_f}$: The total number of loading cycles until the complete failure of the part (the index “f” comes from the English word failure).

$\boldsymbol{N_{in}}$**:** The number of cycles required to initiate a fatigue crack.

$\boldsymbol{N_{pr}}$: The number of cycles required to propagate the crack until the complete failure of the part.

The Sf constraint, also known as fatigue strength, represents the value of the alternating component Sa in Equations (a) and (b) corresponding to the number of cycles N_f required to cause fatigue failure of the component.

According to Lee et al. (2005), the initial investigations into material fatigue were conducted by August Wohler between 1852 and 1870. As a tribute to this German engineer, the Sf versus N_f curves are referred to as Wohler curves in French-speaking countries. In English-speaking countries, these curves are known as S-N curves.

According to Budynas & Nisbett (2008), the endurance limit of steel can be estimated in the following manner:

$$S_n = \begin{cases} 0.5S_u & (Pour\ S_u \leq 1400\ MPa) \\ 700MPa & (Pour\ S_u > 1400MPa) \end{cases} \quad \text{(II.8)}$$

Some materials do not have an endurance limit. The Wöhler curves of aluminum alloys show no plateau. Consequently, it is common to define S_e as the constraint Sf corresponding to a certain number of cycles N_f, for example 10^6 or 10^7. Even with this definition, the material can fail due to fatigue after the application of 10 load cycles [31]. Very high cycle fatigue is often referred to as gigacycle fatigue.

In general, the fatigue tests are carried out until the complete failure of the specimen rather than until the appearance of a macroscopic crack. This means that Wöhler curves often have N_f rather than Nin on the x-axis.

$$S = \sigma'_f (2N_f)^b \quad \text{(II.9)}$$

$\boldsymbol{\sigma'_f}$: is the coefficient of resistance to fatigue of the material (fatigue strength coefficient)

b: is the fatigue strength exponent of the material.

$\boldsymbol{N_f}$: is the number of inversions of the loading to lead the material to the fracture by fatigue (with each inversion of the loading, one has dS/dt = 0)

Basquin's law can be expressed as follows:

$$\log(Nf) = A - B\log(S_f) \quad \text{(II.10)}$$

where the adjustment parameters A and B can be expressed in terms of σ'_f and b:

$$A = -\frac{log(\sigma' f 2^b)}{b} \quad \text{(II.11)}$$

$$B = -1/b \quad \text{(II.12)}$$

Basquin's law was formulated specifically to depict the linear section of the Wöhler curve when plotted on a bi-logarithmic scale. Various alternative models have been put forth to account for the concave sections. One such model is Stromeyer's law (1914), which effectively captures the concavity within the range where Sf approaches Se.

$$\text{Log}(N_f) = A - B \log(S_f - S_e) \quad \text{(II.13)}$$

If there is insufficient experimental data to determine the horizontal asymptote of the curve depicted, the parameter S_e can be treated as a fitting parameter in Equation (5.9), similar to coefficients A and B. In this scenario, when the endurance limit Se is assessed in such a manner, it can be regarded as the outcome of extrapolating experimental data.

The principles established by Palmgren (1924), Weibull (1949), and Stüssi (1955) demonstrate the curvature of the curve not only when the stress amplitude, Sf, approaches the endurance limit, S_e, but also when Sf approaches the ultimate strength, S_u:

Palmgren (1924): $\log(Nf + C) = A - B \log(Sf - S_e)$ (II.14)

Weibull (1949): $\log(Nf + C) = A - B \log\left[\frac{(Sf - S_e)}{(Su - S_e)}\right]$ (II.15)

Stüssi (1955): $\log(Nf) = A - B \log\left[\frac{(Sf - S_e)}{(S_u - Sf)}\right]$ (II.16)

S_u is the tensile strength of the material (the maximum force applied in a tensile test divided by the nominal cross-sectional area of the specimen).

V. The rainflow cycle counting method

Among the various techniques available for counting fatigue cycles, we can mention[59, 60]:

- peak counting (peak count method)
- range-restricted peak count
- peak counting with restricted level (level-restricted peak count method)
- counting of peaks between passages by the mean value (mean-crossing peak count method)
- range counting (range method)
- range-pair count method
- level crossing count method
- PVP method (peak valley pair)

- comptage de cycles hystérétiques
- rainflow method.

Matsuishi and Endo (1968) introduced the rainflow method, which is a technique used to count fatigue cycles. Kondo (2003) states that the rainflow method is considered the most advanced and accurate approach for describing the physical process of fatigue. It is regarded as the cutting-edge technique among cycle counting methods.

developed an algorithm for the rainflow method that uses three points (S_i, S_{i+1}, S_{i+2}) to form two stress ranges (ΔS_1, ΔS_2) that are compared at each iteration. Their algorithm only counts complete cycles, while some algorithms, like the one proposed by ASTM, allow for counting half cycles. According to McInnes & Meehan, the three-point rainflow method is not suitable for real-time cycle counting as it requires knowledge of the complete signal in order to rearrange it before counting. The rearrangement is done in such a way that the stress history starts with the global maximum or minimum point .[61]

The rainflow algorithm, eliminates the need for reorganizing the stress sequence prior to counting. It utilizes a set of four points (S_i, S_{i+1}, S_{i+2}, S_{i+3}) to create three stress ranges (ΔS_1, ΔS_2, ΔS_3) that are compared in terms of their magnitudes during each iteration. This algorithm can also be found in the AFNOR standard from 1993. The magnitudes of the stress ranges are indicated as the extents:

$$\Delta S_1 = S_{i+1} - S_i \quad \text{(II.17)}$$

$$\Delta S_2 = S_{i+2} - S_{i+1} \quad \text{(II.18)}$$

$$\Delta S_3 = S_{i+3} - S_{i+2} \quad \text{(II.19)}$$

The counting rule can be expressed in the following manner: if the absolute value of j times the difference between S_2 and S_1 is less than or equal to the absolute value of j times the difference between S_2 and S_3, then j times the difference between S2 represents a complete cycle of fatigue loading.

VI. Diagrams depicting a constant life pattern

Numerous constant life diagrams have been put forth throughout the 20th century, as demonstrated by the studies conducted by Sendeckyj, Norton, Budynas & Nisbett, and Ince & Glinka. These diagrams enable the utilization of the Wöhler curve while considering the impact of average load stress.[62]

Goodman's diagram (1930) is described by the equation:

$$\frac{S_a}{S_f} + \frac{S_\mathrm{m}}{S_\mathrm{u}} = 1 \quad \text{(II.20)}$$

Sf: is the fatigue strength given by the Wöhler curve.

Gerber's equation (1874) is:

$$\frac{S_a}{Sf} + \left(\frac{S_\mathrm{m}}{S_{ys}}\right)^2 = 1 \quad \text{(II.21)}$$

The equation of Soderberg (1930) is based on the elastic limit of the material S_s

$$\left(\frac{S_\mathrm{a}}{S_f}\right) + \left(\frac{S_\mathrm{m}}{S_{ys}}\right) = 1 \quad \text{(II.22)}$$

$$\left(\frac{S_a}{S_f}\right)^2 + \left(\frac{S_m}{S_{ys}}\right)^2 = 1 \quad \text{(II.23)}$$

Morrow's equation (1968) is based on S_v, the true breaking strength of the material:

$$\frac{S_a}{S_f} + \frac{S_m}{S_v} = 1 \quad \text{(II.24)}$$

S_v takes into account the necking (the reduction in cross-sectional area) of the specimen subjected to the tensile test. It is the value of the tensile force at the moment of failure divided by the cross-sectional area in the constriction zone. Since $S_v > S_u$, Morrow's diagram predicts a longer lifetime than Goodman's diagram.

$$\mathrm{Sf} = \mathrm{S_{max}}^{1-\mathrm{m}}\mathrm{S_a}^{\mathrm{m}} \quad \text{(II.25)}$$

$$\mathrm{S_f} = \mathrm{S_{max}}\left(\frac{1-R_\mathrm{s}}{2}\right)^{\mathrm{m}} \quad \text{(II.26)}$$

$$S_f = \mathrm{S_a}\left(\frac{2}{1-R_\mathrm{s}}\right)^{1-\mathrm{m}} \quad \text{(II.27)}$$

The parameter 'm' in the equation is a fitting parameter based on experimental data and is dependent on the material being studied. This parameter, referred to as the Walker exponent, is also present that represents the rate at which a fatigue crack propagates.

The constant life diagram devised by Heywood is obtained by: [35]

$$\left(\frac{S_a}{S_u}\right) = \left(1 - \frac{S_m}{S_u}\right)\left[\frac{S_f}{S_u} + \varphi\left(1 - \frac{S_f}{S_u}\right)\right] \quad \text{(II.28)}$$

$$\varphi = \left(\frac{S_m}{3S_u}\right)\left(2 + \frac{S_m}{S_u}\right) \quad \text{(II.29)}$$

$$\varphi = \left(\frac{S_m}{S_u}\right)\left[1 + \left(\frac{S_u log(N_f)}{2200}\right)^4\right]^{-1} \quad \text{(II.30)}$$

represents stresses in units of MPa, while Nf denotes the number of cycles corresponding to Sf on the Wöhler curve. The Heywood curve exhibits similarities to the Goodman curve when Sf greatly exceeds the endurance limit Se, but resembles the Gerber curve when Sf approaches Se, experimental findings tend to fall between the Goodman and Gerber curves in most cases.

Figure II. 4 compares diagrams of Goodman, Soderberg, Gerber and ASME elliptical for S355 steel. According to Jesus et al. this steel has a Sys yield strength of 355 MPa and a tensile strength S_u of 470 MPa. The fatigue resistance S_f considered is 213 MPa at 10 million cycles, given by $S_f = 952;2(2N_f - 0;089)$. We see that the Soderberg diagram leads to a more conservative project, since it produces the smallest area where life is greater than 10^7 cycles.[63]

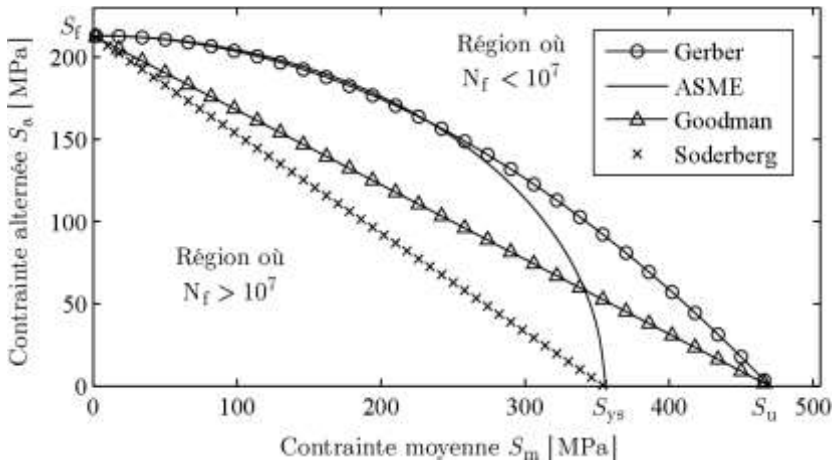

Figure II . 2: Comparison of constant life diagrams for S355 steel

VII. Accumulation of damage

The utilization of the Palmgren-Miner law allows for the quantification of fatigue damage in situations where the loading exhibits varying amplitudes. The law's formula is expressed as follows:

$$D = \sum_{i=1}^{K} \frac{n_i}{N_{fi}} = \sum_{i=1}^{K} D_i \quad \text{(II.31)}$$

- **D**: The overall measure of damage.
- **D_i**: The harm linked to the set of loads characterized by a stress level equivalent to S_{fi}.
- **ni:** The number of counted cycles whose stress level is equal to S_{fi}.

- **N_{fi}:** The Wöhler curve provides the number of cycles needed to fracture the part when subjected to a stress level S_{fi}.

The Palmgren-Miner law operates under the premise that damage accumulation follows a linear pattern. When considering two identical loading cycles occurring at different times within a lengthy history of varying stress levels, the Palmgren-Miner law states that these cycles will result in equivalent damage, irrespective of preceding cycles or the current state of damage in the component. This law assumes the feasibility of categorizing loading cycles based on S_f values. The number of loading groups or blocks is denoted by the variable "k".[64]

If the tests to obtain the Wöhler curve have been carried out until complete rupture of the specimen, complete rupture of the part analyzed can be expected when the damage parameter D reaches the value 1.0.

The crack becomes visible when D reaches a critical value Dc which will be close to zero if the material is purely brittle and close to 1.0 if the material is purely ductile. For most materials, $0.2 \leq Dc \leq 0.5$ [65]

The uniaxial critical damage parameter can be evaluated according to:

$$D_{1c=1} - \frac{S_{nr}}{S_u} \tag{II.32}$$

The nominal breaking stress S_{nr} in a tensile test refers to the stress at which the specimen fails, calculated by dividing the force applied to the specimen at the time of failure by the nominal cross-sectional area.

VIII. The evaluation of damage using the Dirlik method

The probability density function PR(Sf) introduced by Dirlik (1985), is utilized to forecast the outcomes of cycle counting using the rainflow method based on the Power Spectral Density (PSD) of the stress signal.

$$P_R(S_f) = \frac{\frac{d_1}{Q} exp\left(-\frac{Z}{Q}\right) + \frac{d_2}{R^2} exp\left(-\frac{Z^2}{2R^2}\right) + d_3 Z\, exp\left(-\frac{Z^2}{2}\right)}{\sqrt[2]{m_0}} \tag{II.33}$$

$$d_1 = \frac{2(x_m - \gamma^2)}{1+\gamma^2} \tag{II.34}$$

$$d_2 = \frac{1-\gamma-d_1+{d_1}^2}{1-R} \tag{II.35}$$

$$d_3 = 1 - d_1 - d_2 \tag{II.36}$$

$$Q = \frac{1.25(\gamma - d - dR)}{d} \tag{II.37}$$

$$R = \frac{\gamma - x_m - {d_1}^2}{1 - \gamma - d_1 + {d_1}^2}$$

$$Z = \frac{S}{2\sqrt{m_0}} \quad ; \quad \gamma = \frac{m_2}{\sqrt{m_0 m_4}} \quad ; \quad x_m = \frac{m_1}{m_0}\sqrt{\frac{m_2}{m_4}}$$

In these equations, x_m is the average frequency and γ is the irregularity factor, which can also be evaluated according to:

$$\gamma = \frac{E[0]}{E[\rho]} \tag{II.38}$$

assesses E[0], which represents the frequency of stress signal sign changes per second. Evaluates E[ρ], indicating the count of signal peaks occurring per second: [37]

$$E[0] = \sqrt{\frac{m_2}{m_0}} \tag{II.39}$$

$$E[\rho] = \sqrt{\frac{m_4}{m_2}} \tag{II.40}$$

According to the given information, the evaluation of the kth order spectral moment can be carried out as follows:

$$m_k = \int_0^\infty n^k S(n) dn \tag{II.41}$$

n: The frequency is measured in Hertz, while S_n represents the power spectral density function of the stress signal.

The damage D can be evaluated by: [35]

$$D = \frac{E[\rho]\,\Delta t}{10^A} \int_{S_1}^{S_2} {S_f}^B \, P_R(S_f)\, dS_f \tag{II.42}$$

Δt: The duration associated with the damage D is denoted as the time period. Basquin's law, expressed determines the values of the exponents A and B. The integration boundaries S1 and S2 represent the range in which the Wöhler curve is applicable.

IX. Conclusion

mechanical fatigue and stress equations play a vital role in understanding and predicting the behavior of materials under various loading conditions. These equations provide valuable insights into the endurance and structural integrity of components and systems subjected to repetitive or fluctuating loads.

The fatigue equation, often expressed through S-N curves, helps engineers determine the fatigue life of a material by relating the applied stress (S) and the number of cycles to failure (N). This relationship enables them to assess the durability of a component and make informed decisions regarding its design and application.[66]

On the other hand, stress equations, such as Hooke's Law and various failure criteria, aid in quantifying the internal forces and deformations experienced by a material. By analyzing stresses and strains, engineers can identify potential failure points, optimize designs, and ensure that components operate within safe operating limits.

Understanding the interplay between fatigue and stress is crucial for developing reliable and long-lasting structures, machines, and devices. By accounting for the effects of cyclic loading and stress concentration, engineers can mitigate the risks of fatigue failure and enhance the overall performance and longevity of materials and systems.

Furthermore, advancements in computational techniques and material science have led to the development of more sophisticated models and simulations, allowing for accurate predictions of fatigue life and stress behavior. These tools facilitate the optimization of designs, material selection, and maintenance strategies, thereby minimizing the potential for catastrophic failures and maximizing the operational efficiency of engineered systems.

In summary, mechanical fatigue and stress equations serve as fundamental tools for engineers in analyzing and predicting the performance of materials under various loading conditions. Their application is crucial for ensuring the safety, reliability, and durability of structures and components, contributing to advancements in technology, engineering, and innovation.

CHAPTER III

MACHINE CONCEPTION AND DESIGN

I. Introduction

Three-dimensional design, has revolutionized the way we visualize and create objects, spaces, and concepts. Unlike traditional two-dimensional design, which is confined to width and height, 3D design adds depth to the equation, allowing for a more comprehensive and immersive representation of ideas.

In the realm of 3D design, objects are no longer limited to flat surfaces; they gain volume, structure, and the ability to be viewed from various angles, mimicking the way we perceive the physical world. This technology has transcended its initial application in fields like architecture and engineering, branching into diverse sectors such as animation, gaming, product development, and even medical imaging.

The advent of sophisticated software tools has propelled 3D design to new heights, enabling designers to model intricate shapes, simulate real-world physics, and bring their imaginative visions to life. With the aid of these tools, artists, engineers, and creators can manipulate virtual objects, explore design alternatives, and communicate ideas more effectively.

In this document, we explored the development of a contemporary apparatus with the intention of evaluating the strain experienced by wind turbine blades. This was achieved through the utilization of the renowned software "SOLIDWORKS”, which facilitated the creation of three-dimensional representations. This approach not only nurtured creativity but also accommodated significant machine-specific insights.

II. machine parts:

II.1 lower part of base

Of course, we realize that any piece or object has multiple faces and angles according to the overall design, curvature and other geometries. From this point, we will proceed to the explanation.

As shown in the image below, the shape of the base for our particular machine is shown, as well as the dimensions we based it on.

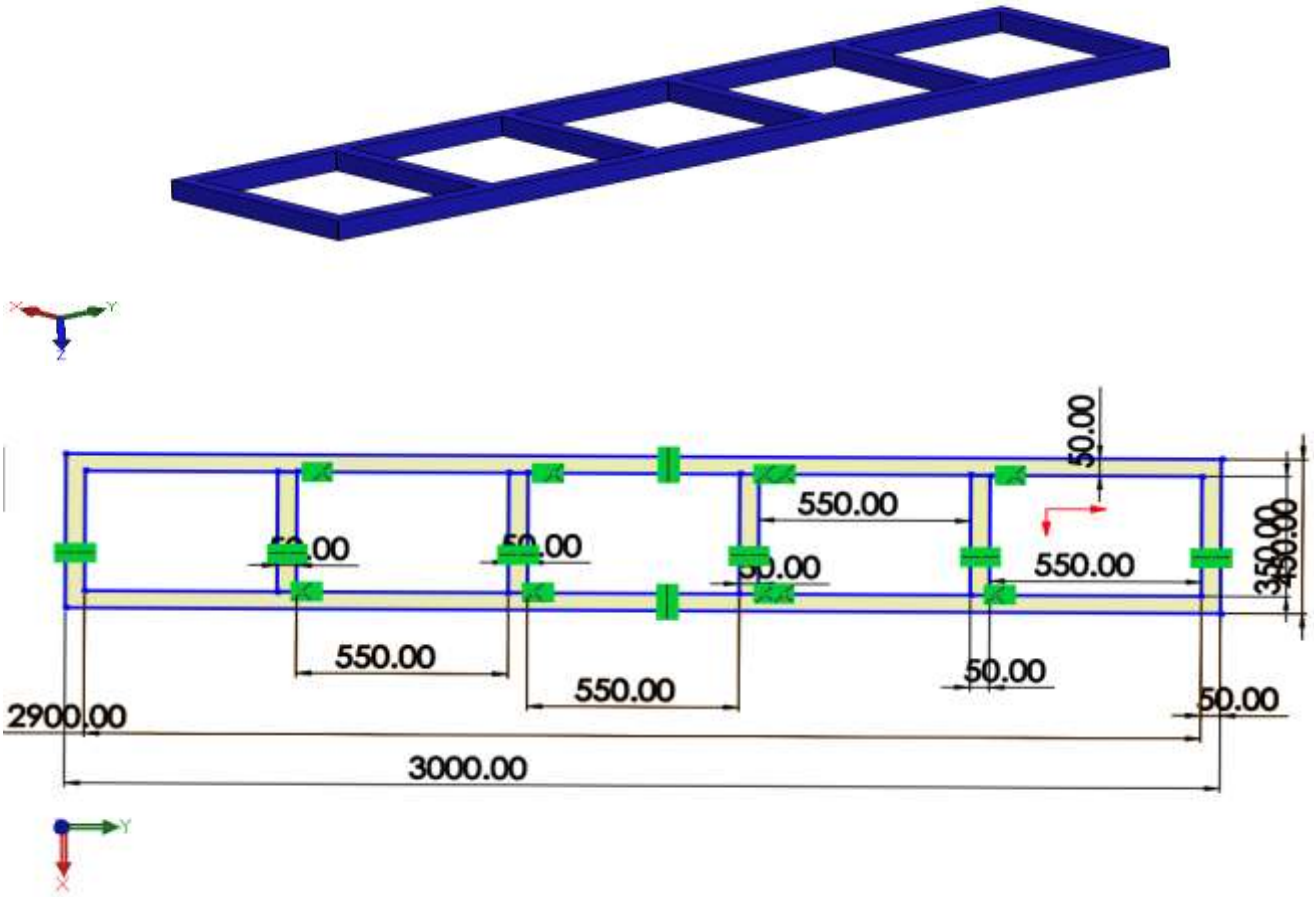

Figure III . 1: Machine base with dimensions

II.2 vertical side part of base

In this section, we created a rectangular component accompanied by an additional piece that is secured using screws. This piece serves as the point of attachment for our blade, as illustrated in the diagram.

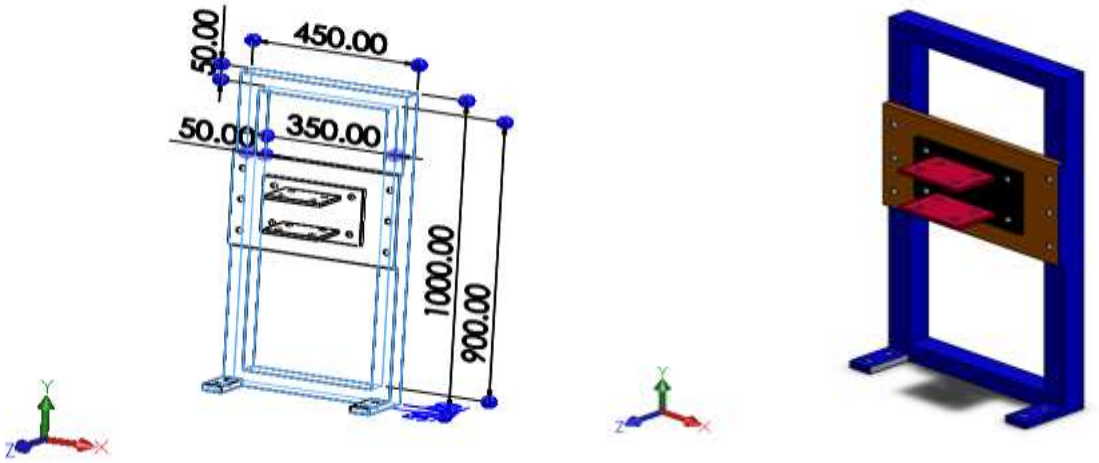

Figure III. 2: Side part with dimensions

We collect these two parts to form one piece like this.

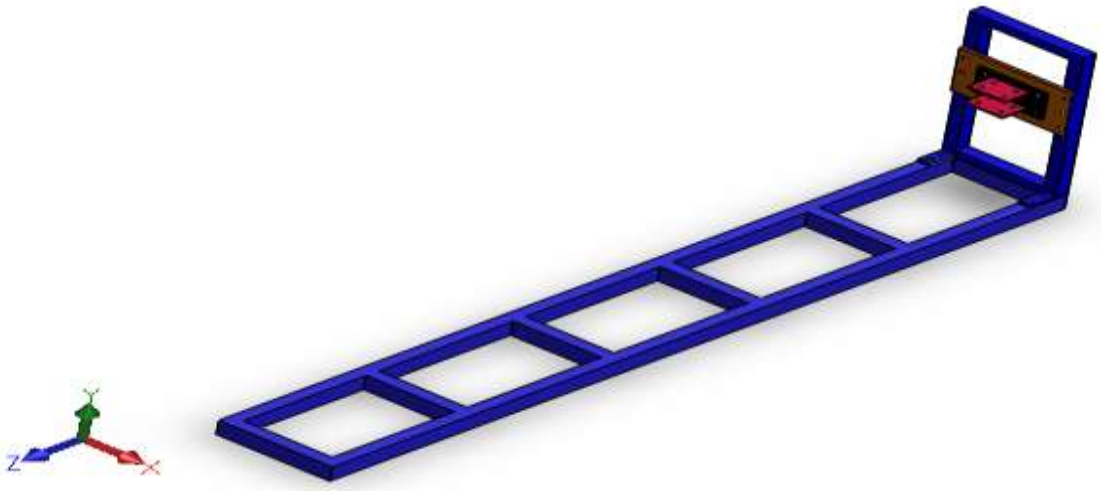

Figure III . 3: Combine the base with the side part

II.3 The engine

In our design, we use a 5.5-horsepower engine as a proposed option for experimentation, and it changes with the change of the extracted data and measurements in reality, as shown in the figure.

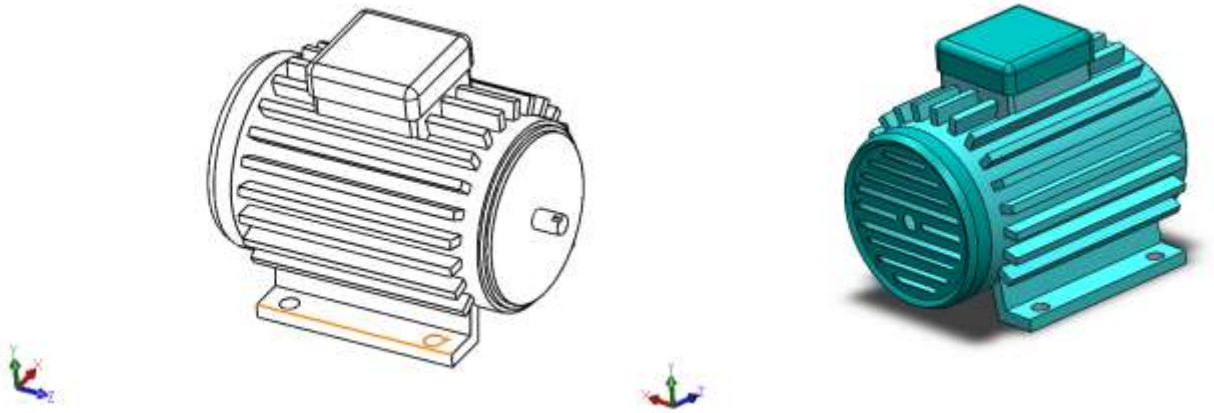

Figure III . 4:power engine

II.3.1 Moving rule

We design an iron plate to install the motor on it to facilitate movement on the base as shown in the following figure

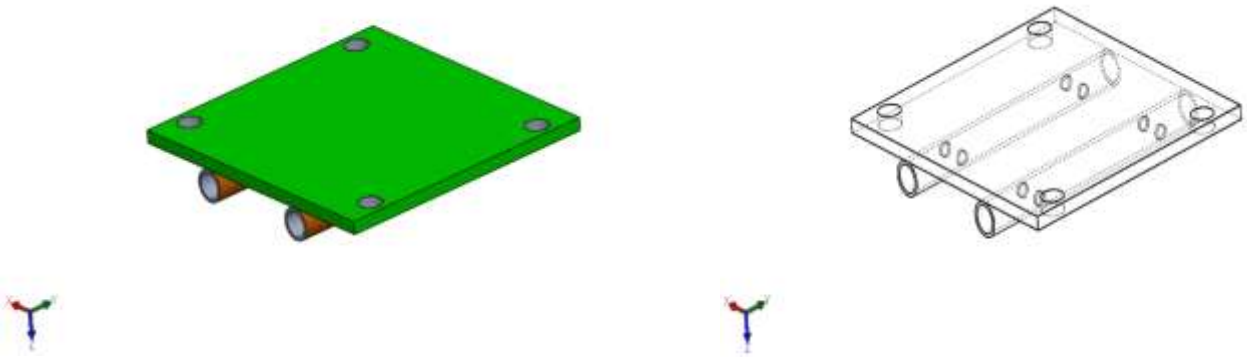

Figure III . 5: Iron plate to install the motor

We add screws on the sides to curb the movement of the plate and install the motor at the point we want.

At the bottom, we install 13-gauge screws to install the motor base at any point we want

II.3.2 Boli

We install this piece on the front face of the engine as show in the following figure

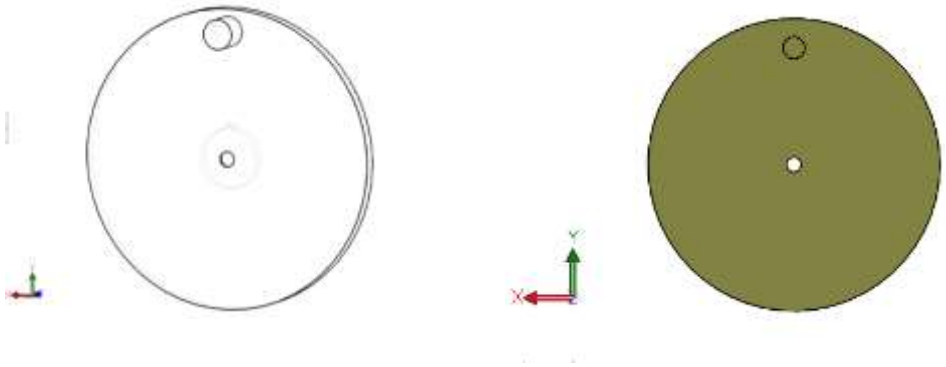

Figure III . 6: Install Boli on the engine

In this piece, we connect an arm connected to a sensor device above, as shown in the following figure

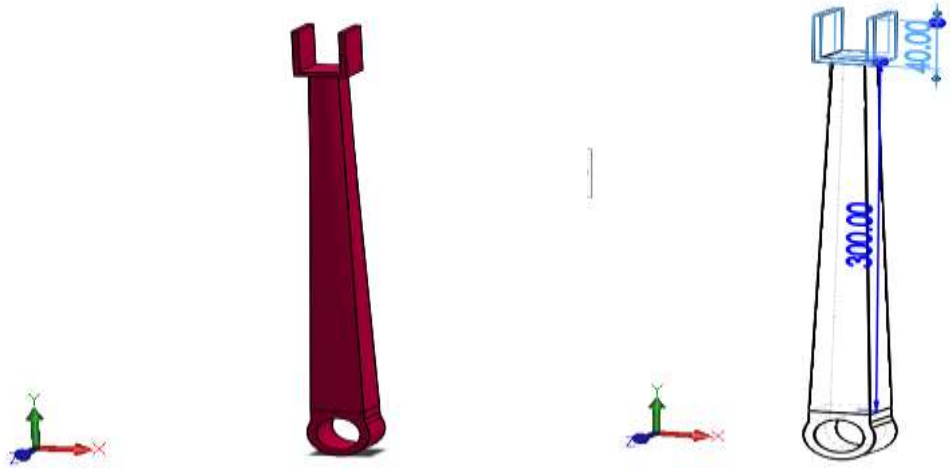

Figure III . 7: Iron arm

II.3.3 loads sensor

A device used to measure the force or loads applied to a specific surface and convert it into an electrical signal or a signal that can be read and analysed. This device is used in a wide range of applications, from industrial technologies to medical and consumer electronic applications.

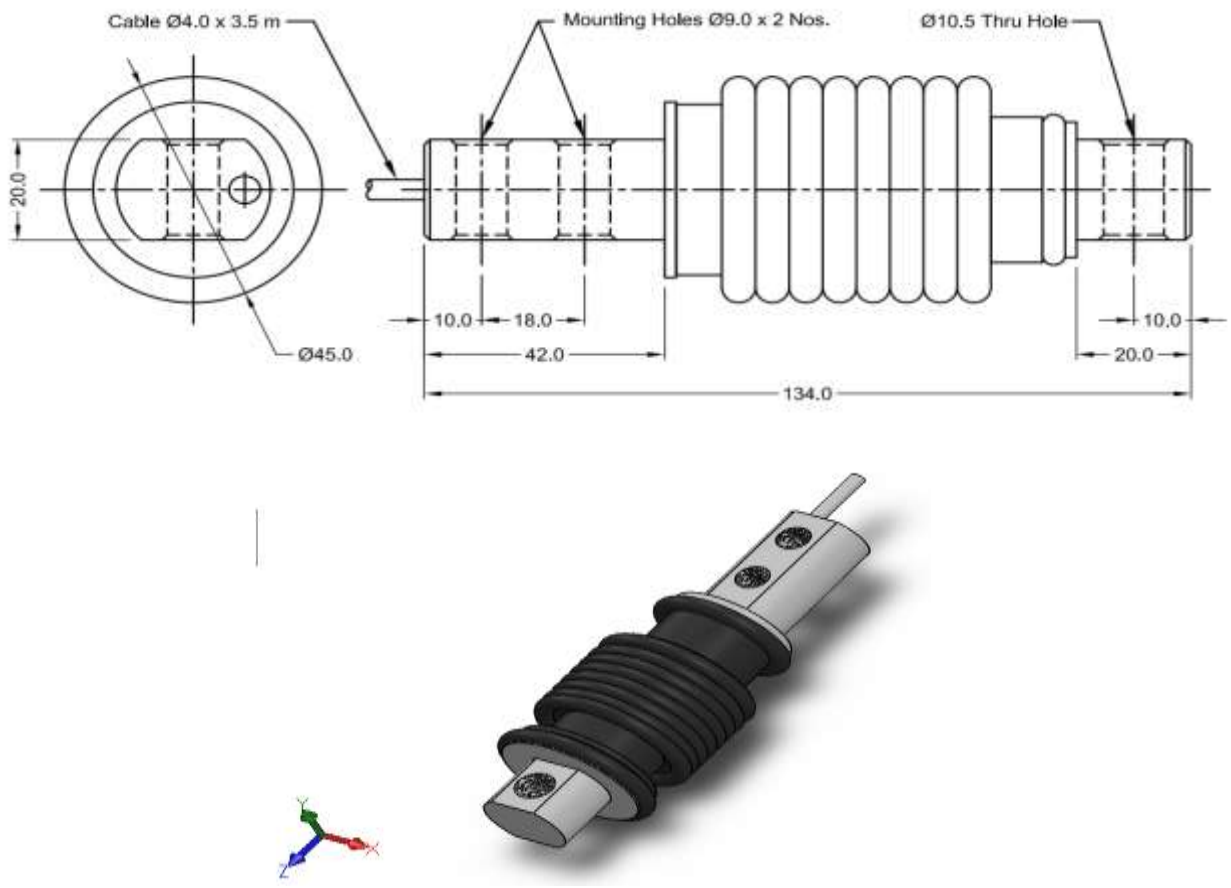

Figure III . 8: Load sensor with dimensionless design

By completing the required pieces of the machine, we collect them as shown in the following figure

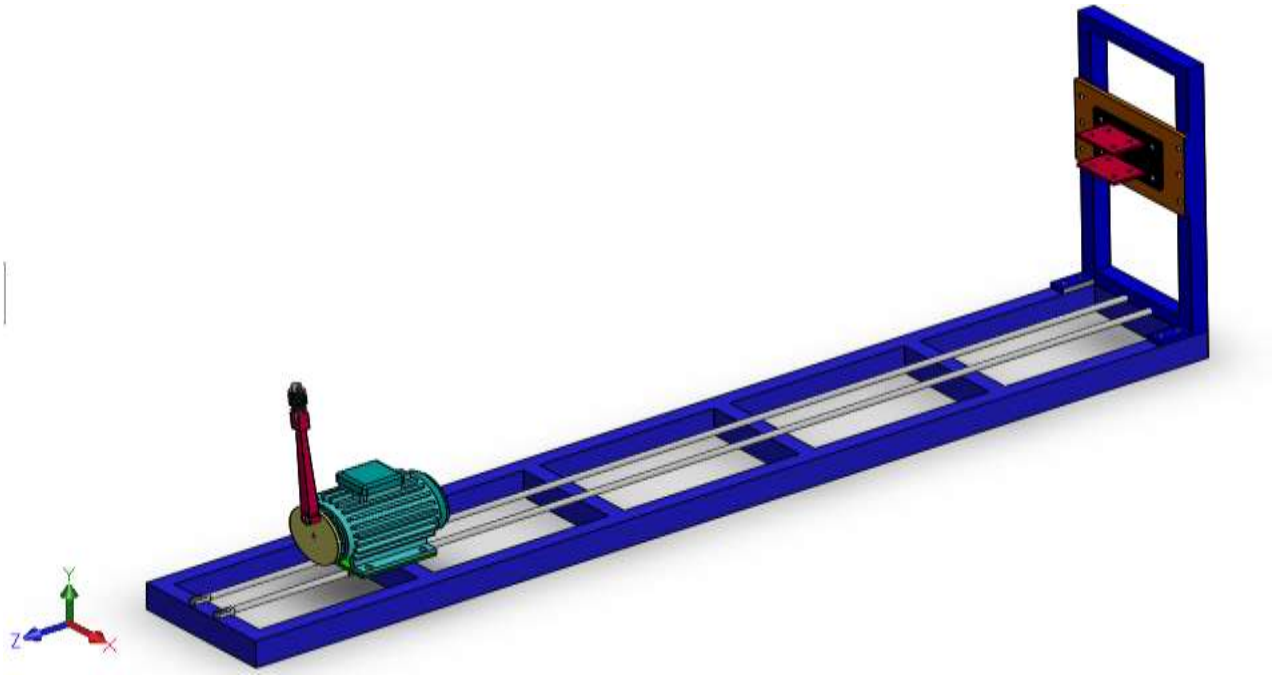

Figure III . 9: Assembly of machine parts

We install the blade in place from the front and back ends separately and on a specific surface as shown in the final figure

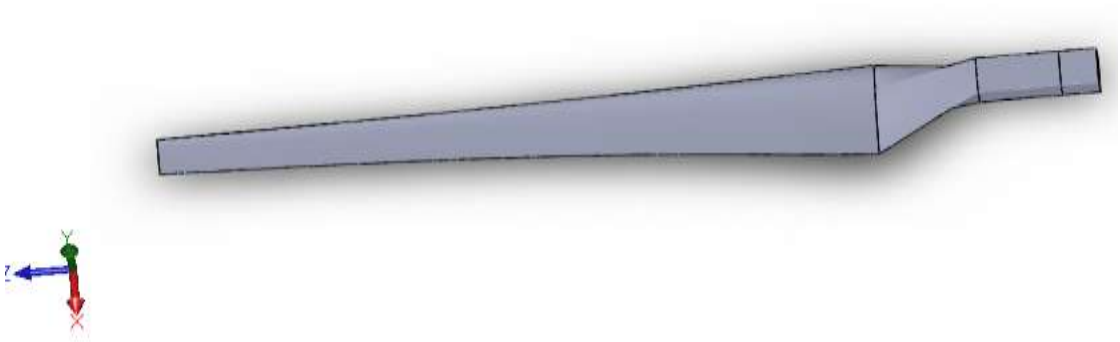

Figure III . 10: The blade of 2.5m used

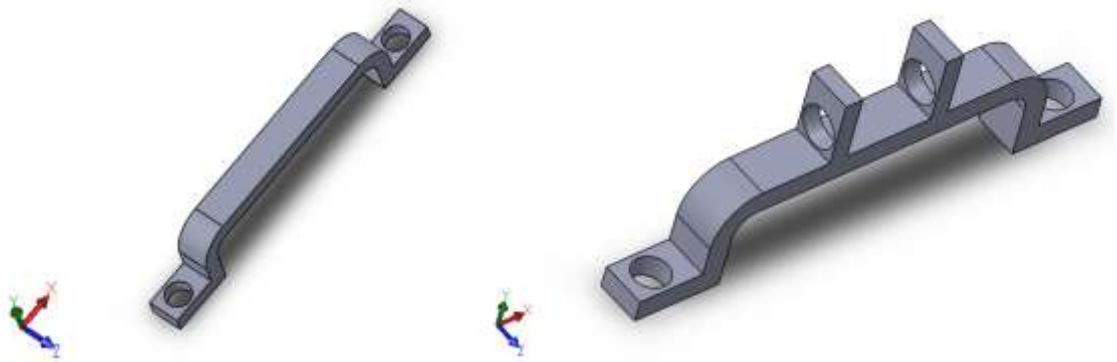

Figure III . 11: Handles used to hold the blade

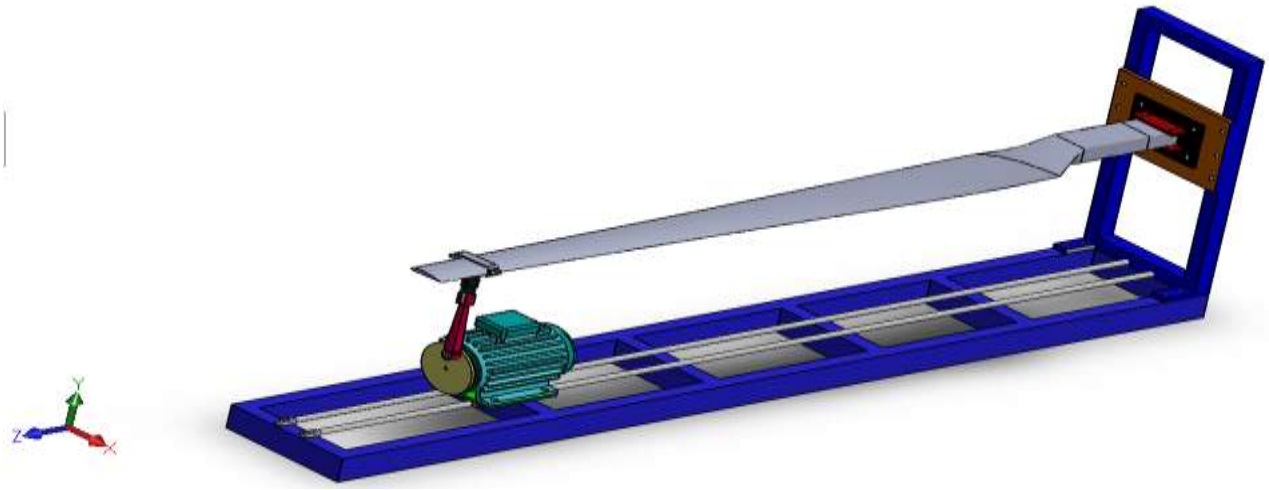

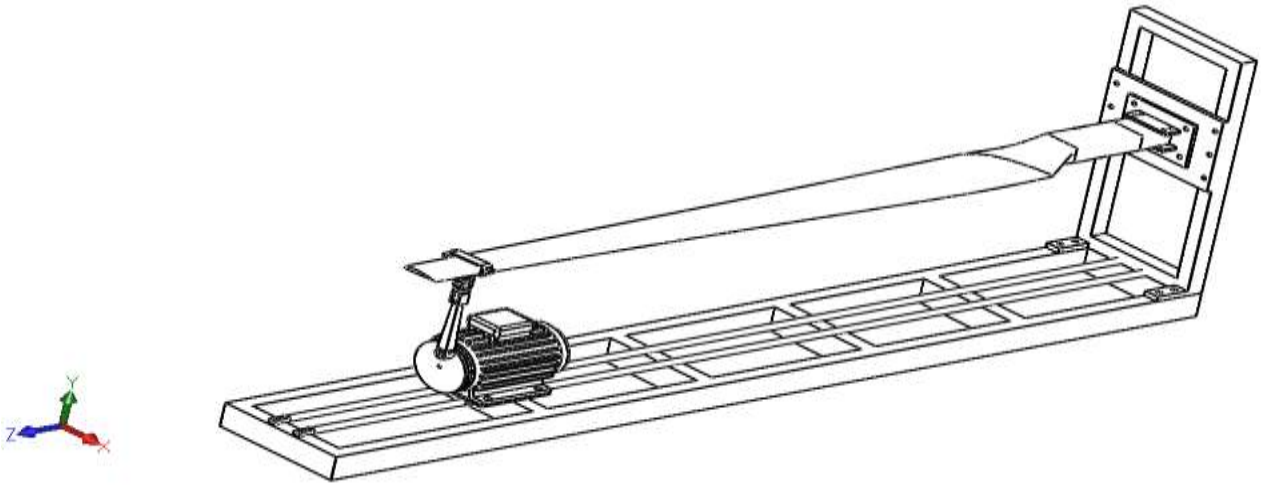

Figure III. 12: The final shape of the machine

When the motor rotates and the blade is withdrawn, we test the extent to which it can withstand the voltage applied to it at different intensities and record it. Based on that, we study the appropriate standards for a strong and long-lasting blade.

III. Machine tests simulation

The simulation process aims to analyze the structure of the machine and deduce areas of weakness in the structure by applying different loads to study stresses and displacement.

III.1 Import design

In this step, we convert the machine design into an IGS file and then export it to the Ansys program to begin the simulation process.

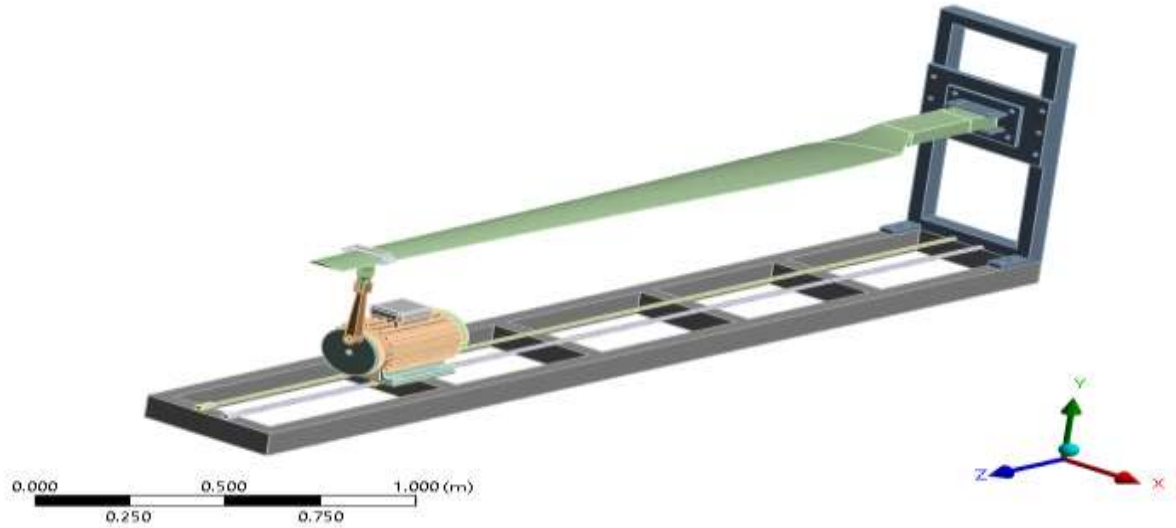

Figure III . 13: Preparing the machine to start the simulation process.

III.2 Machin mesh

In the mesh stage, all pieces of the machine are divided into a group of nodes and small elements, and the mesh is updated after each result until we reach a difference that does not exceed 5 % between the results. The final number of nodes for the simulation is 407,440 and the number of elements is 147,307. We relied on a tetrahedron element with 10 nodes for each element.

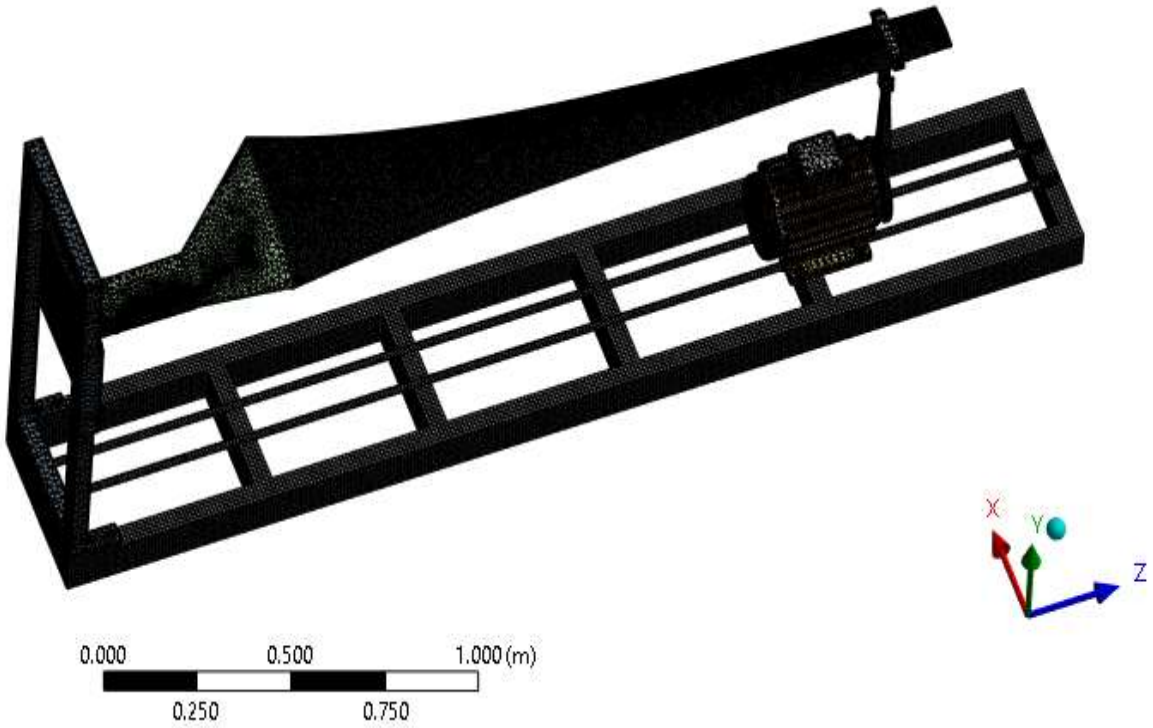

Figure III. 14: Dividing all parts of the machine into a set of nodes and small elements

III.3 Boundary conditions

As can be seen in the figure below, the limit conditions are to install the machine from the bottom in the area of contact with the ground and to apply the load of the motor's workplace or the loads applied by the motor.

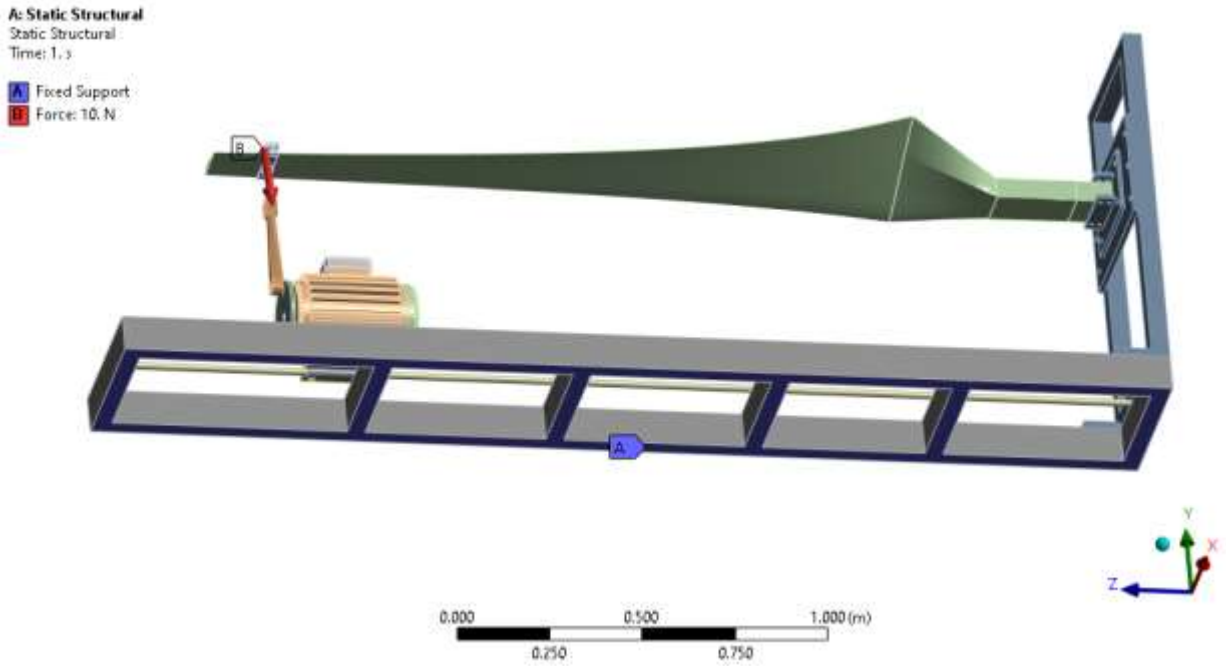

Figure III . 15: Limit conditions for the machine

IV. Machine analyses results

In the beginning of the analysis, we will hide the parts that are subject to constant change so that we can notice the stresses on the fixed parts, such as the motor and the base.

IV.1 The von mises stress

Von Mises stress analysis is adopted to determine the area most exposed to pressure during the operation phase. Therefore, the area where the stresses are high will be the first place to be exposed to breakage or failure. As can be seen in Figure 10, the stresses are concentrated on the engine rollers, as they are the area that is exposed to pressure due to the loads. As for the rest of the structure, the effect of the load will be almost non-existent.

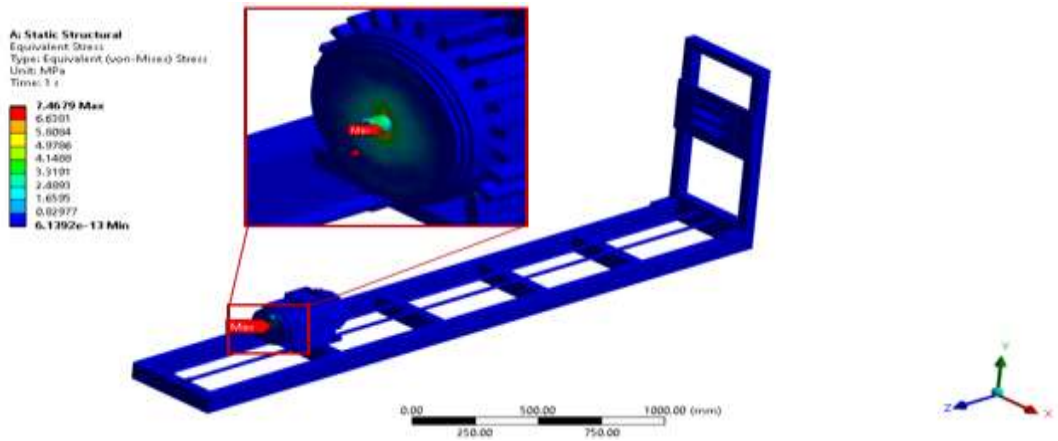

Figure III . 16: Von Mises stress analysis

As is clear, the maximum stress to which the rollers will be exposed is about 7.46 MPa, and this will not cause them to fail because the stress causing failure of the rollers must be more than 4000 MPa according to ISO 74.

IV.2 Machine deformation

Deformation is considered one of the main reasons for mechanical parts to lose their function, causing the mechanical system to malfunction with each other. Therefore, we will analyze the deformation to see which mechanical parts will be exposed to it and whether the deformation will affect the performance of its function.

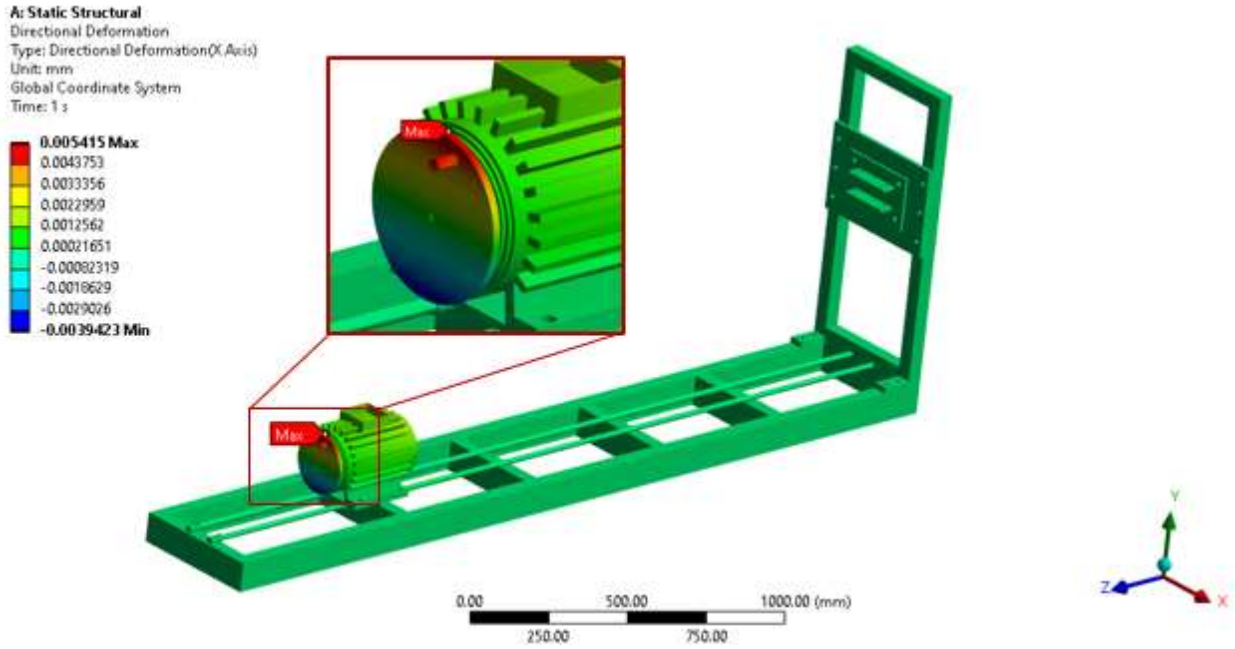

Figure III . 17: Deformation analysis

As can be seen in Figure 17, the highest value of deformation was 0.005 mm, which is a very small value if we consider the amount of expansion of the material, which means that it will not cause any problems to the mechanical part and will maintain its function for a long period of time.

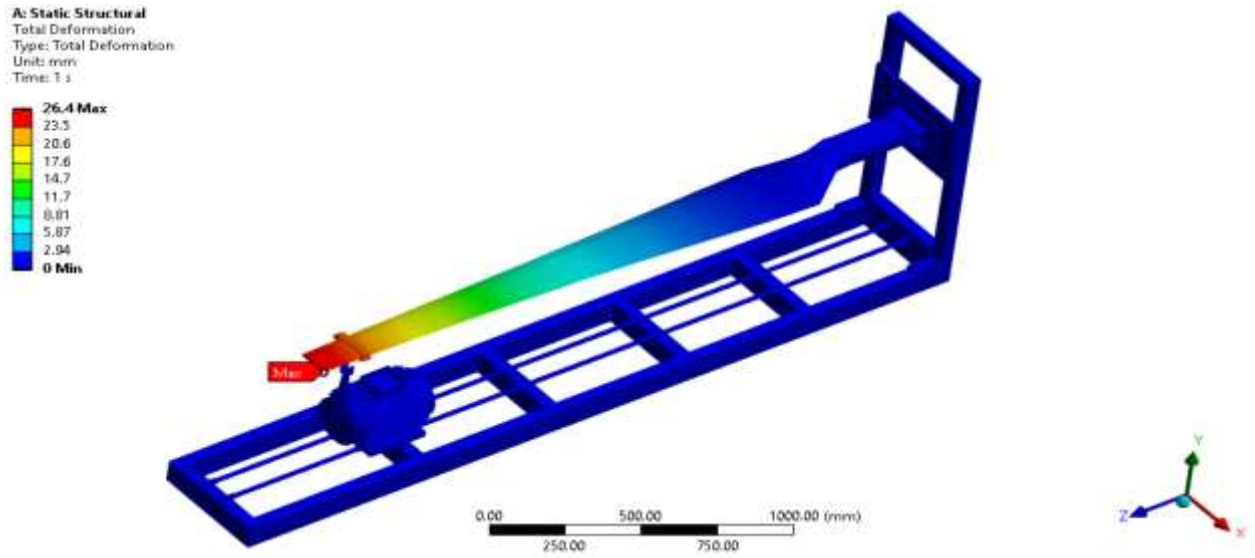

Figure III . 18: Analysis of the entire system of the machine

It is also clear from the analysis of the entire system in Figure 18 that the maximum deformation will be to the blade, while the designed machine will not have any deformation in its structure, as it is clear that the deformation is non-existent, because the blade manufacturing material is less durable and susceptible to deformation before the designed machine material, which makes it succeed in the process of experimental study of small blades.

V. Conclusion

Wind energy concludes with its prominent importance as a source of renewable energy, as wind power generation devices play a crucial role in converting wind energy into electrical energy. The operation of wind instruments is based on the principles of aerodynamics, where differences in air pressure cause the device blades to rotate due to applied loads. However, cyclic application of these loads over time results in a phenomenon known as fatigue. Fatigue is important for wind instrument blades as it leads to significant material deterioration. To solve this problem, a study was carried out to design a modern device aimed at analyzing the fatigue of wind instrument blades. The main goal of this device is to simplify fatigue studies for researchers, enabling them to better understand the life of wind instrument blades.

GENERAL CONCLUSION

VI. Conclusion General

The study of mechanical fatigue of wind turbines and the design of related machinery is a vital research area that contributes to improving the performance and reliability of renewable energy sources. By understanding the effects of mechanical fatigue on turbine components and related designs, we can improve efficiency and sustainability and reduce costs.

The study of mechanical fatigue of wind turbines includes several important aspects, such as stress and strain analysis in the main components of the turbine, such as blades, bearings and wind turbines. It is necessary to evaluate how factors such as strong winds and weather changes affect the turbine and how it can be designed to withstand these stresses well.

In addition, the mechanical fatigue study includes potential damage assessment and maintenance forecasting, so that maintenance efforts can be directed more effectively and unplanned downtimes avoided.

The design of machinery and technology related to wind turbines must take into account all factors related to mechanical fatigue, and this requires continuous innovation and improvement in designs, materials and methods. The development of technology in this field contributes to making wind turbines more effective in terms of exploiting the wind and reducing costs, and this enhances their contribution to generating clean and sustainable electricity.

In conclusion, the study of mechanical fatigue and machining design of wind turbines plays a crucial role in developing renewable energy technology and improving environmental and economic sustainability. These research and efforts continue to advance renewable energy and achieve environmental mitigation goals to meet the world's growing electricity needs.

Reference

[1] T. Burton, N. Jenkins, D. Sharpe, and E. Bossanyi, *Wind energy handbook*. John Wiley & Sons, 2011.

[2] A. Greco, S. Sheng, J. Keller, and A. Erdemir, "Material wear and fatigue in wind turbine systems," *Wear,* vol. 302, no. 1-2, pp. 1583-1591, 2013.

[3] J. Marin, A. Barroso, F. París, and J. Cañas, "Study of fatigue damage in wind turbine blades," *Engineering failure analysis,* vol. 16, no. 2, pp. 656-668, 2009.

[4] H. Mughrabi and S. D. Antolovich, "A tribute to Claude Bathias–Highlights of his pioneering work in Gigacycle Fatigue," *International Journal of Fatigue,* vol. 93, pp. 217-223, 2016.

[5] Q. Demassieux, B. Huneau, E. Verron, and D. Berghezan, "Investigation of mode III fatigue crack growth in rubber based on the pioneering work of Alan N. Gent and coworkers," *International Journal of Non-Linear Mechanics,* vol. 68, pp. 25-32, 2015.

[6] C. R. Doering and J. D. Gibbon, *Applied analysis of the Navier-Stokes equations* (no. 12). Cambridge university press, 1995.

[7] S. Bhat and R. Patibandla, "Metal fatigue and basic theoretical models: a review," *Alloy steel-properties and use,* vol. 22, 2011.

[8] A. Saxena, J. Landes, and J. Bassani, "Nonlinear fracture mechanics. Volume 1. Time-dependent fracture," 1989.

[9] P. C. Paris, H. Tada, and J. K. Donald, "Service load fatigue damage—a historical perspective," *International Journal of fatigue,* vol. 21, pp. S35-S46, 1999.

[10] P. Agreement, "Report of The Conference of The Parties on Its Twenty-First Session, Held in Paris from 30 November to 13 December 2015," FCCC/CP/2015/10/Add. 1, United Nations, European Commision Secretariate, 2015.

[11] A. Savaresi, "The Paris Agreement: a new beginning?," *Journal of Energy & Natural Resources Law,* vol. 34, no. 1, pp. 16-26, 2016.

[12] C. Streck, P. Keenlyside, and M. Von Unger, "The Paris Agreement: a new beginning," *Journal for European Environmental & Planning Law,* vol. 13, no. 1, pp. 3-29, 2016.

[13] N. Kirthika, K. Ramachandran, and S. K. Kottayil, "Deep quantile regression based wind generation and demand forecasts," in *Proceedings of the 11th International Conference on Soft Computing and Pattern Recognition (SoCPaR 2019) 11*, 2021: Springer, pp. 112-122.

[14] E. D. Delarue, P. J. Luickx, and W. D. D'haeseleer, "The actual effect of wind power on overall electricity generation costs and CO2 emissions," *Energy conversion and management,* vol. 50, no. 6, pp. 1450-1456, 2009.

[15] C. D. Hanning and A. Evans, "Wind turbine noise," vol. 344, ed: British Medical Journal Publishing Group, 2012.

[16] E. Pedersen and K. Persson Waye, "Perception and annoyance due to wind turbine noise—a dose–response relationship," *The Journal of the Acoustical Society of America,* vol. 116, no. 6, pp. 3460-3470, 2004.

[17] P. Gulve and S. B. Barve, "Design and construction of vertical axis wind turbine," *International Journal of Mechanical Engineering and Technology (IJMET),* vol. 5, no. 10, pp. 148-155, 2014.

[18] W. Tjiu, T. Marnoto, S. Mat, M. H. Ruslan, and K. Sopian, "Darrieus vertical axis wind turbine for power generation II: Challenges in HAWT and the opportunity of multi-megawatt Darrieus VAWT development," *Renewable Energy,* vol. 75, pp. 560-571, 2015.

[19] A. R. Winslow, "Urban wind generation: comparing horizontal and vertical axis wind turbines at Clark University in Worcester, Massachusetts," 2017.

[20] A. Shires and V. Kourkoulis, "Application of circulation controlled blades for vertical axis wind turbines," *Energies,* vol. 6, no. 8, pp. 3744-3763, 2013.

[21] B. I. Brill, "Modular wind energy device," ed: Google Patents, 2002.

[22] "Types of wind turbines." Energy Education. https://energyeducation.ca/ (accessed.

[23] M. M. A. Bhutta, N. Hayat, A. U. Farooq, Z. Ali, S. R. Jamil, and Z. Hussain, "Vertical axis wind turbine–A review of various configurations and design techniques," *Renewable and Sustainable Energy Reviews,* vol. 16, no. 4, pp. 1926-1939, 2012.
[24] M. Ragheb, "Vertical axis wind turbines," *University of Illinois at Urbana-Champaign,* vol. 1, no. 40, 2011.
[25] M. Zemamou, M. Aggour, and A. Toumi, "Review of savonius wind turbine design and performance," *Energy Procedia,* vol. 141, pp. 383-388, 2017.
[26] "Savonius wind turbine." wikipeadia. https://en.wikipedia.org/ (accessed.
[27] M. Jiménez Portaz, "Experimental study of the interaction of natural and man-made exploitation systems with the environment in the atmospheric surface boundary layer: Application to olive fields and wind farms," 2021.
[28] "An innovative small-scale power plant generates environmentally friendly energy in Gerlingen." Energy from a wind tree. https://www.endress.com/ (accessed.
[29] A. Wind, "Horizontal Axis Wind Turbines (HAWT) with Case Studies."
[30] L. Du, G. Ingram, and R. G. Dominy, "A review of H-Darrieus wind turbine aerodynamic research," *Proceedings of the Institution of Mechanical Engineers, Part C: Journal of Mechanical Engineering Science,* vol. 233, no. 23-24, pp. 7590-7616, 2019.
[31] M. Islam, D. S. K. Ting, and A. Fartaj, "Aerodynamic models for Darrieus-type straight-bladed vertical axis wind turbines," *Renewable and Sustainable Energy Reviews,* vol. 12, no. 4, pp. 1087-1109, 2008/05/01/ 2008, doi: https://doi.org/10.1016/j.rser.2006.10.023.
[32] M. M. M. Saad and N. Asmuin, "Comparison of horizontal axis wind turbines and vertical axis wind turbines," *IOSR Journal of Engineering (IOSRJEN),* vol. 4, no. 08, pp. 27-30, 2014.
[33] "Horizontal Axis Wind Turbine," *ScienceDirect* 2020. [Online]. Available: https://www.sciencedirect.com/.
[34] P. J. Moriarty and A. C. Hansen, "AeroDyn theory manual," National Renewable Energy Lab., Golden, CO (US), 2005.
[35] M. T. REALITY. "3D Rendering "Helukabel"." CAD-LAIF. https://www.cad-laif.com (accessed.
[36] W. F. UPDATE. "Belgium's Largest Offshore Wind Farm Officially Inaugurated." Adnan Durakovic. https://www.offshorewind.biz (accessed 10 Oct, 2021).
[37] K. Anup, J. Whale, and T. Urmee, "Urban wind conditions and small wind turbines in the built environment: A review," *Renewable energy,* vol. 131, pp. 268-283, 2019.
[38] W. Wisatesajja, W. Roynarin, and D. Intholo, "Comparing the effect of rotor tilt angle on performance of floating offshore and fixed tower wind turbines," *J. Sustain. Dev,* vol. 12, pp. 84-95, 2019.
[39] M. Karimirad and C. Michailides, "V-shaped semisubmersible offshore wind turbine: An alternative concept for offshore wind technology," *Renewable Energy,* vol. 83, pp. 126-143, 2015.
[40] R. Antonutti, C. Peyrard, L. Johanning, A. Incecik, and D. Ingram, "An investigation of the effects of wind-induced inclination on floating wind turbine dynamics: heave plate excursion," *Ocean Engineering,* vol. 91, pp. 208-217, 2014.
[41] M. Collu and M. Borg, "Design of floating offshore wind turbines," in *Offshore wind farms*: Elsevier, 2016, pp. 359-385.
[42] R. Farrugia, T. Sant, and D. Micallef, "A study on the aerodynamics of a floating wind turbine rotor," *Renewable energy,* vol. 86, pp. 770-784, 2016.
[43] J. Kang, L. Sun, H. Sun, and C. Wu, "Risk assessment of floating offshore wind turbine based on correlation-FMEA," *Ocean Engineering,* vol. 129, pp. 382-388, 2017.
[44] "What is mechanical testing: Different types of mechanical testing of materials," ed: RAPID DIRECT, 2022.
[45] "Torsion Testing Machines," ed: ADMET, 2022.
[46] R. H. D. R. O. R. J. K. T. A. M. Brendzel, "Cyclic fatigue and fracture in pyrolytic carbon-coated graphite mechanical heart-valve prostheses: Role of small cracks in life prediction," *Journal of Biomedical Materials Research Part B: Applied Biomaterials,* vol. 28, no. 7, 1994.

[47] D. Vandepitte and P. Sas, "Case study of fracture of a mechanical component due to resonance fatigue," *Mechanical Systems and Signal Processing,* vol. 4, no. 2, pp. 131-143, 1990.
[48] T. Ackermann and L. Söder, "Wind energy technology and current status: a review," *Renewable and sustainable energy reviews,* vol. 4, no. 4, pp. 315-374, 2000.
[49] G.-J. Cho, C.-H. Kim, Y.-S. Oh, M.-S. Kim, and J.-S. Kim, "Planning for the future: Optimization-based distribution planning strategies for integrating distributed energy resources," *IEEE Power and Energy Magazine,* vol. 16, no. 6, pp. 77-87, 2018.
[50] M. Kwon *et al.*, "Overview of KSTAR initial operation," *Nuclear Fusion,* vol. 51, no. 9, p. 094006, 2011.
[51] C. S. Kong, K. H. Kim, J. S. Choi, J. E. Kim, C. Park, and J. W. Jeong, "Salicin, an Extract from White Willow Bark, Inhibits Angiogenesis by Blocking the ROS-ERK Pathways," *Phytotherapy research,* vol. 28, no. 8, pp. 1246-1251, 2014.
[52] C. Kong, J. Bang, J. Jeong, M. Kang, S. Jeong, and J. Yoo, "Structural design of medium scale composite wind turbine blade," in *13th International Conference on Composite Materials (ICCM-13)*, 2001, p. 561.
[53] R. Petráš, V. Škorík, and J. Polák, "Thermomechanical fatigue and damage mechanisms in Sanicro 25 steel," *Materials Science and Engineering: A,* vol. 650, pp. 52-62, 2016.
[54] J. Schijve, "Four lectures on fatigue crack growth," Delft University of Technology, 1977. [Online]. Available: http://resolver.tudelft.nl/uuid:704226c6-658f-46b8-8cf4-68eeb56fb45a
[55] K. Miller, "Metal fatigue—past, current and future," *Proceedings of the Institution of Mechanical Engineers, Part C: Mechanical Engineering Science,* vol. 205, no. 5, pp. 291-304, 1991.
[56] S. Khan, A. Vyshnevskyy, and J. Mosler, "Low cycle lifetime assessment of Al2024 alloy," *International Journal of Fatigue,* vol. 32, no. 8, pp. 1270-1277, 2010.
[57] J. Wang *et al.*, "“Thermal charging” phenomenon in electrical double layer capacitors," *Nano letters,* vol. 15, no. 9, pp. 5784-5790, 2015.
[58] K. Ohura, M. Bohner, P. Hardouin, J. Lemaître, G. Pasquier, and B. Flautre, "Resorption of, and bone formation from, new β-tricalcium phosphate-monocalcium phosphate cements: An in vivo study," *Journal of Biomedical Materials Research: An Official Journal of The Society for Biomaterials and The Japanese Society for Biomaterials,* vol. 30, no. 2, pp. 193-200, 1996.
[59] B. Dumas, D. Lalanne, and S. Oviatt, "Multimodal interfaces: A survey of principles, models and frameworks," *Human machine interaction: Research results of the mmi program,* pp. 3-26, 2009.
[60] W. Cheng, J. Outeiro, J.-P. Costes, R. M'Saoubi, H. Karaouni, and V. Astakhov, "A constitutive model for Ti6Al4V considering the state of stress and strain rate effects," *Mechanics of Materials,* vol. 137, p. 103103, 2019.
[61] J. A. Bannantine, *A variable amplitude multiaxial fatigue life prediction method*. University of Illinois at Urbana-Champaign, 1989.
[62] T. Heus, H. J. Jonker, H. E. Van den Akker, E. J. Griffith, M. Koutek, and F. H. Post, "A statistical approach to the life cycle analysis of cumulus clouds selected in a virtual reality environment," *Journal of Geophysical Research: Atmospheres,* vol. 114, no. D6, 2009.
[63] H. Rajabi, A. Darvizeh, A. Shafiei, D. Taylor, and J.-H. Dirks, "Numerical investigation of insect wing fracture behaviour," *Journal of biomechanics,* vol. 48, no. 1, pp. 89-94, 2015.
[64] U. T. Brunk and A. Terman, "The mitochondrial-lysosomal axis theory of aging: accumulation of damaged mitochondria as a result of imperfect autophagocytosis," *European journal of biochemistry,* vol. 269, no. 8, pp. 1996-2002, 2002.
[65] E. Haibach, *Betriebsfeste Bauteile: Ermittlung und Nachweis der Betriebsfestigkeit, konstruktive und unternehmerische Gesichtspunkte*. Springer-Verlag, 2013.
[66] L. He, Z. Wang, H. Akebono, and A. Sugeta, "Machine learning-based predictions of fatigue life and fatigue limit for steels," *Journal of Materials Science & Technology,* vol. 90, pp. 9-19, 2021/11/10/ 2021, doi: https://doi.org/10.1016/j.jmst.2021.02.021.